

Paper 7

Remote Sensing for Mineral Exploration – A Decade Perspective 1997-2007

Agar, B. ^[1], Coulter, D. ^[2]

-
1. Affiliation of Author1
 2. Affiliation of Author2

ABSTRACT

The years between 1997 and 2007 saw significant advances in remote sensing technology for mineral exploration. The successful launch of the ASTER instrument in 1999 brought with it the ability to map mineral zoning and quartz occurrences within alteration systems. This took remote sensing from the age of the ambiguous “TM anomaly” into the age of mineral mapping from space. While ASTER has rapidly become the workhorse of geologic remote sensing, high spatial resolution satellite image and high spectral resolution airborne imaging have also advanced. Sub-meter multispectral satellite systems allow near airphoto quality imagery to be acquired anywhere in the world. The “open skies” policy of the satellite operators permits high resolution image acquisitions to be undertaken in locations where it was not possible before. Although slower to be embraced by the exploration community, airborne hyperspectral data that is capable of mapping individual mineral species and chemical substitutions within individual minerals has progressed to the point of being an operational commercial technology. With the improvements in spectral resolution have come advances in the processing of the remote sensing data. The results of remote sensing data analysis have progressed from highly qualitative anomaly identification to quantitative mineral species mapping.

INTRODUCTION

Remote sensing is often the first technology applied to exploration projects – few geologists would now visit a prospect without first “Google-Earthing” (Wikipedia 2007) it. In early stage exploration, ASTER (Advanced Spaceborne Thermal Emission and Reflection Radiometer) imagery provides a synoptic view of potential alteration and alteration zoning in exposed terrains at very low cost. Remote sensing technology is the only remote exploration method that directly maps the broad range of alteration minerals associated with many ore deposits. In many ways, remote sensing is the modern equivalent of an experienced prospector with a good sense of field indicator minerals of alteration and mineralization. More importantly, modern remote sensing methods allow us to quantify the alteration mineralogy and identify key pathfinder minerals and chemical variations within minerals that are invisible to even the most seasoned exploration geologist.

The last decade has seen significant advances in remote sensing technology. Satellite systems have evolved to provide higher spatial and spectral resolutions critical for mineral exploration. Sub-meter pixel satellite imagery allows near aerial photographic quality color images to be acquired anywhere on the planet. Web based compilation of imagery through services such as Google Earth permit desktop access to imagery that was

inconceivable in the 90's. Analog aerial photographic acquisition and compilation itself has almost completely been supplanted by digital photography. The ASTER earth resources satellite instrument and airborne hyperspectral imagery permit the mapping of mineral families, mineral species, and even chemical substitutions within individual minerals. The processing of remote sensing data has advanced from the generation of qualitative anomaly maps to quantitative inversion to mineral maps. Manual interpretation of the remote sensing results on printed maps is rapidly giving way to full digital integration of the data and the use of GIS and statistical based analysis and interpretation.

This paper provides an overview of the current state of remote sensing in mineral exploration. The state of the art in 1997 is reviewed and the advances in data acquisition and processing over the last decade are discussed. The focus of this discussion is on the use of remote sensing for the identification of surface mineralogy. Thus, sensors in the visible to thermal infrared and processing applicable to this region receive emphasis.

Remote sensing is generally described as the measurement of reflected or emitted electromagnetic radiation (EMR) in the range of about 300 nanometers (nm) to 1 meter (m) in wavelength. Earth remote sensing scientists categorize this into several ranges based on the physical interaction phenomena. The visible to near infrared (VNIR) range is reflected EMR dominated by electronic processes that produce broad

absorptions. The shortwave infrared (SWIR) is reflected EMR dominated by molecular vibration processes that produce sharp absorptions. The thermal infrared (TIR) is emitted and some reflected EMR that is also dominated by molecular vibration processes that produce both sharp and broad absorptions. All of these measurements have the sun as an energy source (although the TIR actually has a component that is the Earth's heat). The Sun is an incoherent source of energy; we cannot measure the phase of the response, only the amplitude. Radars in the range of about 1 mm to 1m and utilizes an active source from which both phase and amplitude may be measured. Radar methods are a transition between optical remote sensing and electromagnetic methods. The primary phenomenon that impacts Radar measurements is the molecular rotation (polarization) effect.

In all remote sensing measurements, we are concerned about the amount of energy that is reflected from the surface material. A so-called Lambertian reflector has a reflection that does not depend on wavelength and is spectrally flat. Fortunately, many materials absorb energy at specific wavelengths and possess distinctive spectral signatures that uniquely identify them

(Figure 1). These regions of selective absorption are called absorption features. In the case of high spectral resolution instruments such as hyperspectral imagers (HSI) we can very accurately identify surface minerals. With lower spectral resolution multispectral imagers (MSI) we can identify general classes of minerals or materials. The spectroscopic signature of a material is analogous to color but extends into invisible parts of the electromagnetic spectrum. Just as a geologist may use color to help identify a mineral, we use very precise measurements of "color" to identify minerals remotely.

In the remote sensing study of mineralized systems we have a very fortunate situation: many of the minerals associated with hydrothermal alteration possess highly distinctive spectral signatures. Remote sensing may, therefore, be used to directly detect and map the mineralogy of exposed hydrothermal alteration. The primary limitation of remote sensing is that the surface penetration is only on the order of a few microns. This restricts remote sensing to the arid and semi-arid regions of the Earth where rocks and soils are directly exposed on the surface.

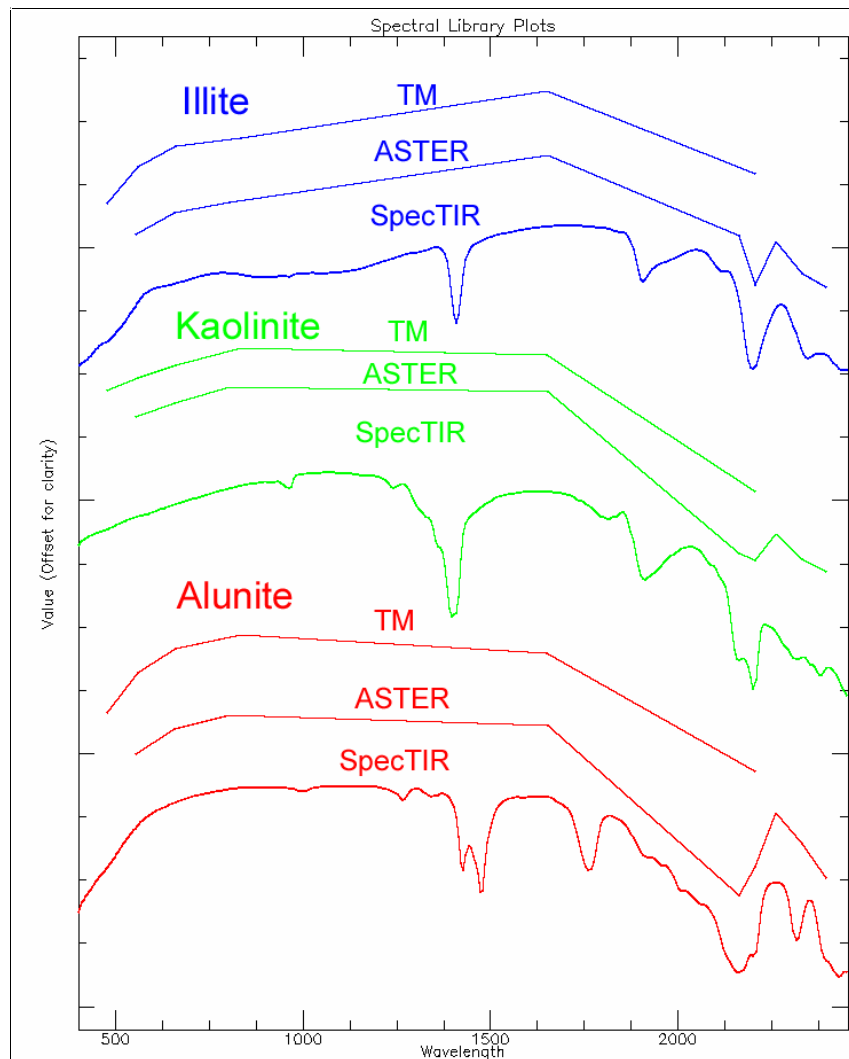


Figure 1: Comparisons of the spectral signatures of alunite, kaolinite, and illite as measured by the TM, ASTER, and SpecTIR sensors.

Background – State of the Art in 1997

After a decade that saw the development of airborne multi-spectral sensors such as Geoscan MKII and the Geophysical and Environmental Research Corporation (GER) DAIS69, only the latter and the short lived multispectral Japanese Earth Resources Satellite (JERS) and hyperspectral Airborne Visible/Infrared Imaging Spectrometer (AVIRIS) were available for data collection in 1997. With costs of airborne data capture relatively high and availability low, the exploration community relied almost exclusively on Thematic Mapper (TM) data for mapping geology and alteration on regional scales.

The typical approaches to the analysis of remote sensing data for exploration in the 90's were the calculation of color ratio composite images (CRC), the use of principal component analysis (PCA) or directed principal component analysis (DPCA), and to a lesser extent, supervised classification (Lipton, 1997). The method of calculating ratios between image bands was first used for earth remote sensing by Rowan et al. (1974) on ERTS-1 (Landsat 1) imagery for mapping lithology and alteration. The method enhances the differences in band responses that are indicative of absorption features (Figure 1). Band ratios are fairly robust for high albedo (brightness) materials commonly seen in alteration systems but are often ambiguous in multispectral data due to the fact that broad band widths may encompass multiple mineral absorptions. Ratio images are highly impacted by atmospheric scattering and a path radiance correction (PRC) must be carefully undertaken to remove scattering effects. Scattering effects may also be minimized by calculation of the difference of logarithms rather than simple division (Pratt, 2001). Principal component analysis of images had its roots in the desire for data compression. The method is a linear projection of the image vector space to a new set of orthogonal vectors that are ranked in decreasing variance. For 4-band Multispectral Scanner (MSS) data, the first three PC images contain the majority of the image information and the fourth PC image is discarded. Unfortunately, subtle geologic information may have a low variance signature and be discarded with the theoretical "noise". This phenomenon of "throwing out the baby with the bath water" became much more critical with 7-band TM data. In addition, the PCA method is data directed and therefore scene dependent. Thus, it does not produce consistent results scene to scene. In order to deal with the limitation of PCA, and the problem of separating mineral signatures from vegetation in Landsat imagery, a method of Directed Principal Components (DPCA) was developed by Crosta and Moore (1989) and further refined by Loughlin (1991).

This method utilizes band and spatial subsets to optimize the separation of materials of interest by "directing" the statistics of the PC calculation. In the case of mapping clay for example, a simple band ratio of band 5 divided by band 7 would enhance not only clays but also vegetation. By using a PCA of bands 3, 4, 5 and 7, the statistics would show which of the 4 principal component bands mapped vegetation and which mapped clay. The PC in which the eigen values for bands 3 and 4 were of opposite sign and large would be mapping vegetation whereas the clay would be mapped in the PC in which the eigen values for bands 5 and 7 were opposite sign and large (Loughlin, 1991).

Iron minerals could also be mapped and "filtered" from vegetation in a similar manner using bands 1, 3, 4 and 5. By the late 90's the "Crosta Method" was the most commonly used approach to enhancing TM data for exploration applications.

An alternative approach for mapping and separating clays from vegetation also uses the covariance statistics of the data and is based upon the close correlation between all bands so that any one band can be modeled from the statistics of the others. Thus, when the clay absorption band (band 7) is modeled using the Least Squares Fit method and the modeled result, is subtracted from the original band 7, the vegetation or predictable component is removed and the residual maps the clay (Fraser & Green, 1987).

As an interesting aside, some of the concepts behind the Crosta method re-immersed as orthogonal sub-space projection methods in the 2000's (Ientilucci, 2001). Classification methods, while effective for categorizing material with high spectral contrasts, were generally found to be ineffective on multispectral data sets for geologic discriminations.

Although not used extensively by the exploration community at the time, airborne hyperspectral imagery (HSI) was beginning to break out of the research arena and into the commercial use sector. HyMap and the similar Probe-1 began acquiring hyperspectral data on a commercial scale in the late 90's. Since HSI was rooted in spectroscopy, spectroscopic analysis tools were already in development for the analysis of HSI data. The Tricorder (now Tetracorder) package from the USGS (Clark et al., 1999) was one of the first spectral analysis tools to be utilized for HSI data. Boardman (1989) also developed methods of inversion based on geophysical signal processing concepts and Kruse et al. (1993) had developed a software package called SIPS (later to become ENVI) that focused on HSI data. The ENVI software package was being used in the commercial arena on airborne multispectral data (Agar & Villanueva, 1997), but its use and that of the airborne data was limited and suffered from the lack of accurate and reliable atmospheric and geometric correction methods.

Although the roots for the application of spectral processing of multi- and hyperspectral data were in place, the almost exclusive reliance on TM data for exploration limited its use. The standard processing methods for multispectral data were all qualitative in nature. Ultimately, a skilled interpreter was needed to make sense of the analysis results and qualitatively (and with much bias) select "real" targets from false anomalies. The term "TM Anomaly" was well entrenched in regional exploration dialog. But things were changing; the next decade saw the growth of quantitative remote sensing.

Data Capture in the 21st Century – Developments in Sensor Technology

Satellite and Airborne Sensors

Although airborne multi- and hyperspectral data were available in 1997 from the Geoscan AMSS MKI and MKII sensors (Agar, 1994), these instruments were no longer operational. The Airborne Visible/InfraRed Imaging Spectrometer (AVIRIS) (JPL, 1987; Vane et al., 1993) was available only on a research campaign basis leaving the GER DAIS-63 sensor (Collins, &

Chang, 1990) as the only one operating commercially. Remote sensing in mineral exploration was still largely focused on Landsat TM data with the application of the higher spatial and spectral resolution data restricted due to a number of factors including the limited number of sensors available; the cost of surveys and mobilization; the difficulty of calibrating and atmospherically correcting the data; and the lack of reliable 3-dimensional spatial location information collected with the data.

AVIRIS required a dedicated aircraft (Sarture et al, 1998) and the GER DAIS63 sensor required installation into an aircraft in the GER hanger in New York State. For both sensors, this meant that surveys outside of the USA or Canada required mobilization of both sensor and aircraft, adding significant importation and logistical costs to the already heavy cost of mobilization. Only in the late 1990's, with instruments such as the De Beers AMS (Hussey, 2004) and subsequent Probe and Hy-Map sensors (Cocks et al., 1998) did the first, truly commercial hyperspectral sensors appear and the instrumentation become sufficiently compact, lightweight. And robust enough to be shipped as freight and then installed onsite in a local aircraft.

The De Beers Airborne Multispectral Scanner was commissioned in 1996 having been designed and built by the Hy-Vista Corporation to specifications determined by De Beers. Hy-Vista subsequently developed additional sensors such as the Probe-1 and 2 and their own Hy-Map sensors (Cocks et al., 1998). Each of these sensors was a "Kennedy" or whisk-broom design, following on from earlier sensor designs used in the Geoscan and the GER-DAIS63.

With the exception of AVIRIS, the new sensors had increased spectral resolution over their predecessors (Figure 2). Where the Geoscan and GER DAIS sensors collected data in 24 and 63 channels respectively, the Hy-Vista sensors recorded information in 128 spectral bands across the same wavelength range. This increased spectral resolution gave the newer instruments far greater capacity to discriminate individual alteration minerals and their variants compared with their airborne and satellite borne predecessors (Figure 3). For example, not only could individual minerals such as illite be mapped, but varieties of illite could now also be discriminated (Figure 4) (Cudahy et al., 2000). Another important and major advantage these new sensors had over their multi-spectral predecessors was that they captured data at wavelengths where absorption due to atmospheric water and other gases could be measured (Figure 2). With the exception of AVIRIS, earlier sensors lacked the ability to collect data at these wavelengths and concentrated on placing their spectral bands in the atmospheric windows. However, by collecting information in the atmospheric water absorption wavelength bands, data from AVIRIS and other new sensors could be used to measure atmospheric moisture on a pixel by pixel basis and so accurately convert the data from radiance to reflectance using newly derived atmospheric models that were at the time being incorporated into commercial remote sensing software packages (Figure 5) (Borel & Schlapfe, 1996; Adler-Golden et al; 1998, Kruse, 1998).

Prior to this, sensors such as Geoscan and the GER DAIS used an internal data normalization process to convert the data to pseudo-reflectance or used input from field spectra collected from large homogeneous targets, easily identifiable in the

imagery to calibrate and convert the data to reflectance using the empirical line method.

The Geoscan AMSS MKII sensor had a stabilized gyroscopic platform that helped to dampen the effects of air turbulence during data collection. In addition, GPS data were recorded during the flight in order to assist in geocoding the imagery. However, the precise orientation of the aircraft in three dimensions could not be recorded for each pixel and as a result the data required manual geo-referencing to pre-existing images or maps. As accurate as any spectral data products such as alteration mineral maps might have been in a spectral context, they lacked spatial accuracy, especially where the geometric distortions inherent in the airborne data were multiplied by high topographic relief.

The appearance of more accurate civilian GPS and Inertial Navigation System (IMS) technologies coupled to more sophisticated stabilization platforms that accurately record the instantaneous 3-D orientation of the sensor relative to the aircraft and hence ground, it became possible to accurately remove geometric distortions in airborne imagery data of all types. Accurate information about the position and orientation of the instrument combined with accurate, high-resolution digital terrain models, makes it possible to accurately orthorectify airborne remotely sensed imagery. Products derived from these data may be easily integrated with other diverse types of data in Geographic Information Systems, greatly increasing the value and applications of the data themselves.

The need to integrate remote sensing data with other information was greatly appreciated by Texaco who, in 1997, contracted Geophysical and Environmental Research Corporation to develop the Texaco Energy and Environmental Multispectral Imaging Spectrometer (TEEMS) hyperspectral sensor (Prelat & Chang, 1997). The TEEMS system was a significant advance in airborne remote sensing technology in that it collected hyperspectral spectral data in the ultraviolet, visible, near, shortwave and thermal infrared parts of the electromagnetic spectrum as well as synthetic aperture radar (SAR) data simultaneously from the same platform. The SAR data were used to provide digital terrain models for structural geological mapping and to which the image data could be orthorectified.

While the Visible-Near Infrared (VNIR) and Short Wave Infrared (SWIR) data provided the same capabilities as the other new sensors such as the Hy-Map series for example, the combined hyperspectral SWIR and multi-spectral Thermal Infrared (TIR) data sets in the TEEMS allowed mapping of silicate mineralogy, quartz and garnet, in particular along with the other hydrothermal alteration minerals. Previously, although the GER DAIS and Geoscan AMSS sensors both had thermal infrared modules, only the Geoscan data had demonstrated a capacity to map silica and skarn mineralogy (Figure 6) (Agar, 1999; Pavez & Agar, 2001). Although the value of TIR data for skarn and silicate mapping has been further demonstrated by Cudahy et al. (2000) using the Spatially Enhanced Broadband Array Spectrograph System (SEBASS) (Hackwell et al., 1996) which collects information in 128 channels from 7.6–13.5 μm . Over the years, SEBASS was made commercially available, withdrawn, and most recently, made available again.

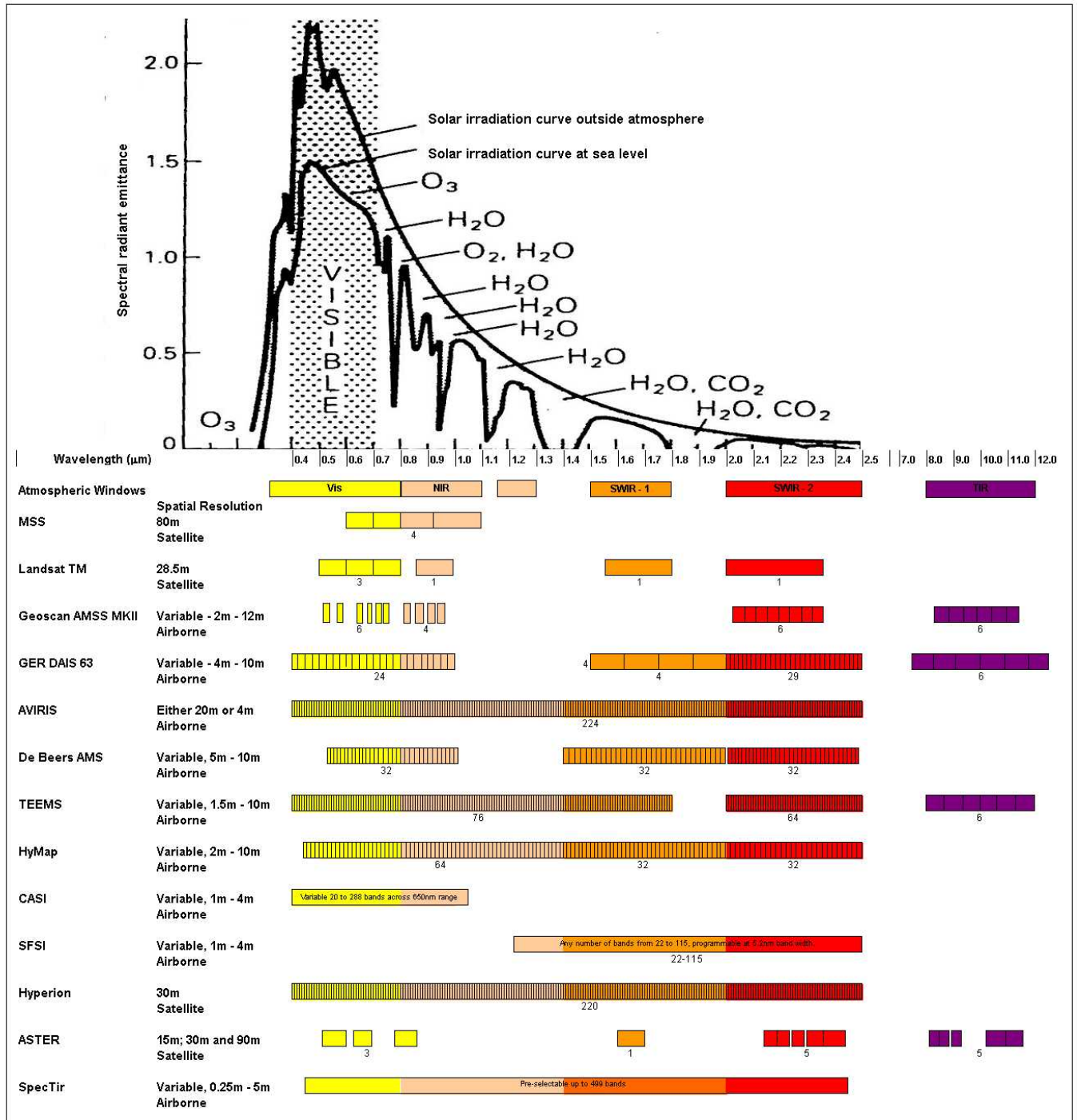


Figure 2: The spatial resolution and spectral band positions of selected sensors plotted relative to incoming solar irradiation, atmospheric absorption and windows.

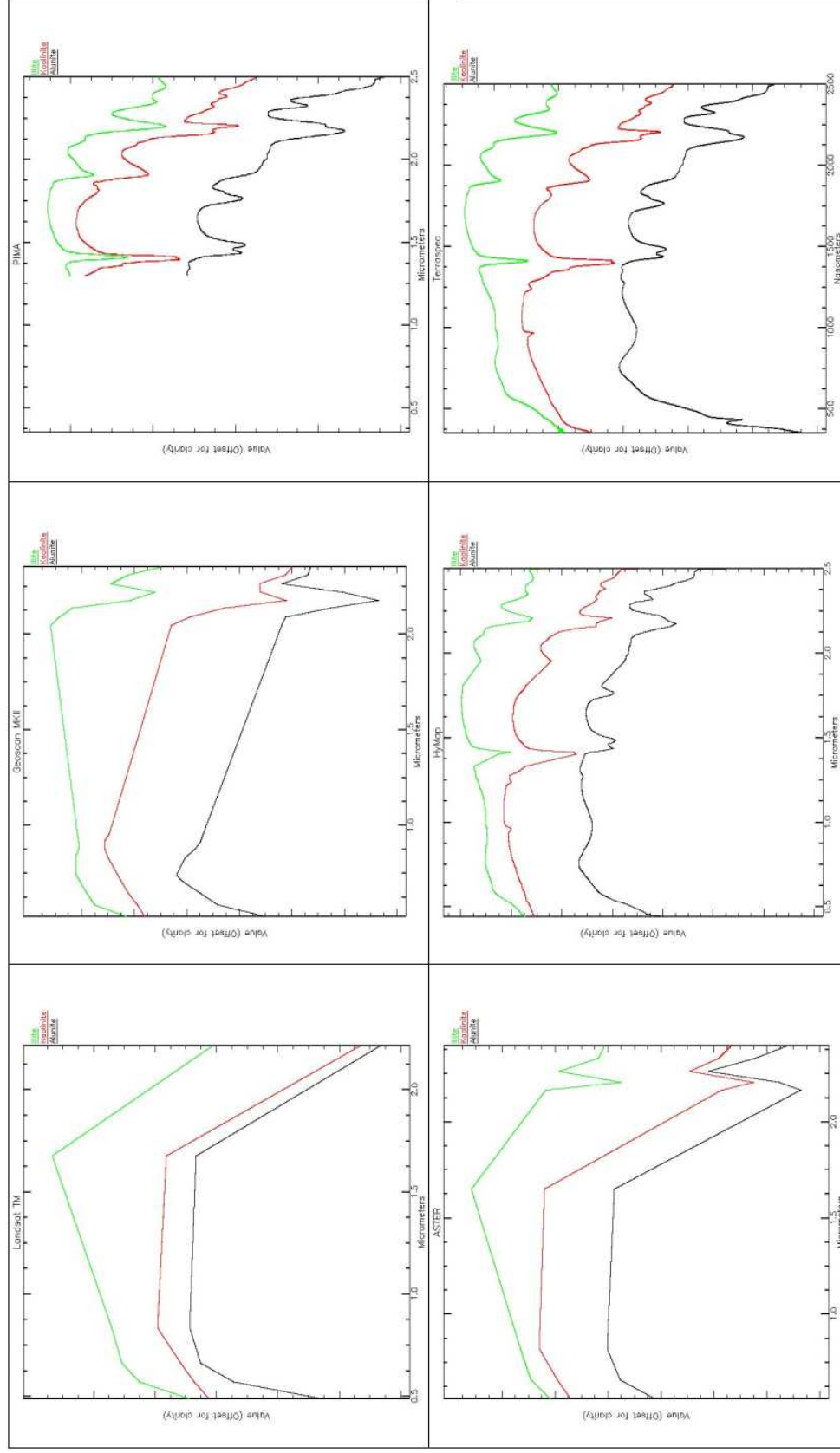


Figure 3: Comparative spectral resolution of data available pre-1997 (top) against recent data (bottom) for satellite-borne sensors (Landsat and ASTER, left), airborne sensors (Geoscan and HyMap, centre) and field spectrometers (PIMA and TerraSpec, right).

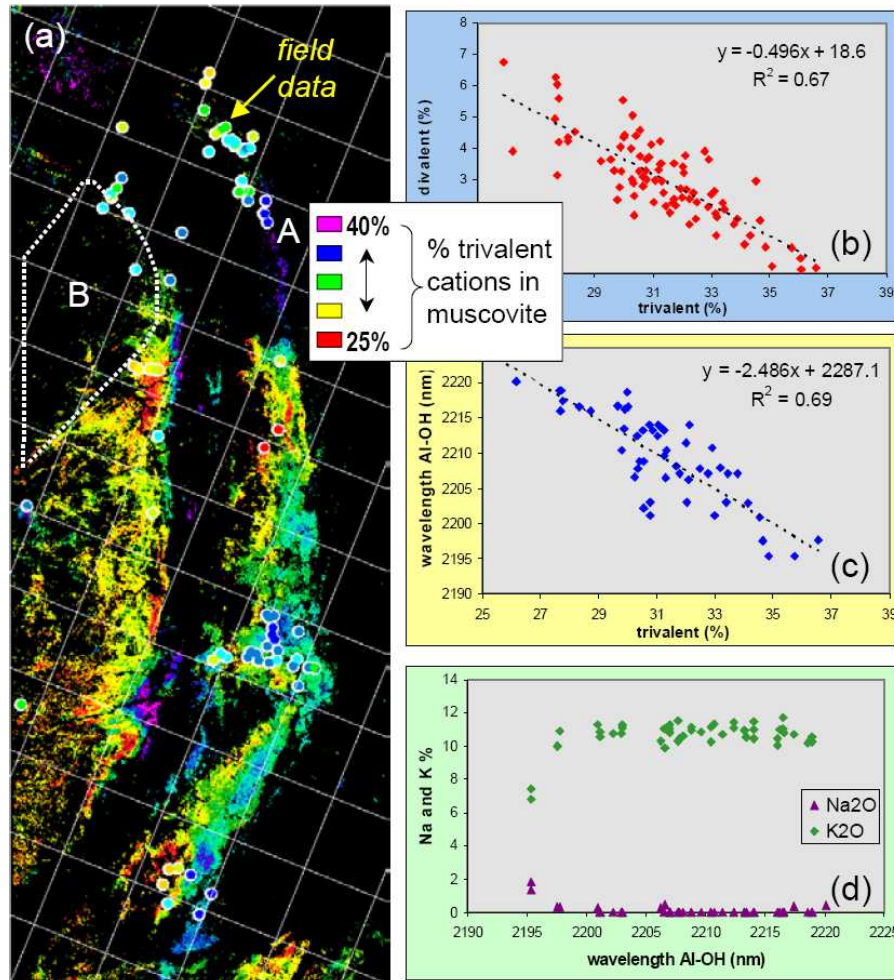


Figure 4: (a) Percentage of trivalent cations within the white mica octahedral layers estimated from HyMap data and PIMA spectra of field samples (coloured circles), Panorama volcanogenic Cu-Zn project, Western Australia; (b) scattergram of electron microprobe white mica analyses of trivalent versus divalent cations; (c) scattergram of electron microprobe white mica analyses of % trivalent cations in the octahedral layer versus the wavelength of the 2200 nm absorption minimum; (d) scattergram of the wavelength of the 2200 nm absorption minimum versus the electron microprobe white mica analyses of % K and Na (after Cudahy et al., 2000).

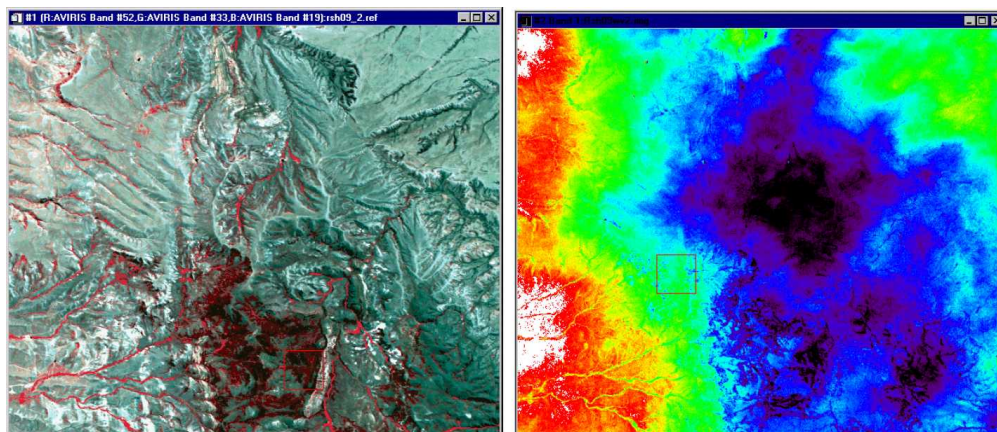


Figure 5: AVIRIS Color Infrared Composite image, Bands 52, 33, and 19 (0.85, 0.67, and 0.55 μm) (RGB)(left) and corresponding color-coded water vapor image (right). The color scale goes from black to blue, to green, to yellow, to red, to white (low column water vapor to high column water vapor). Lower water vapor corresponds with higher elevation areas (after Kruse, 1998).

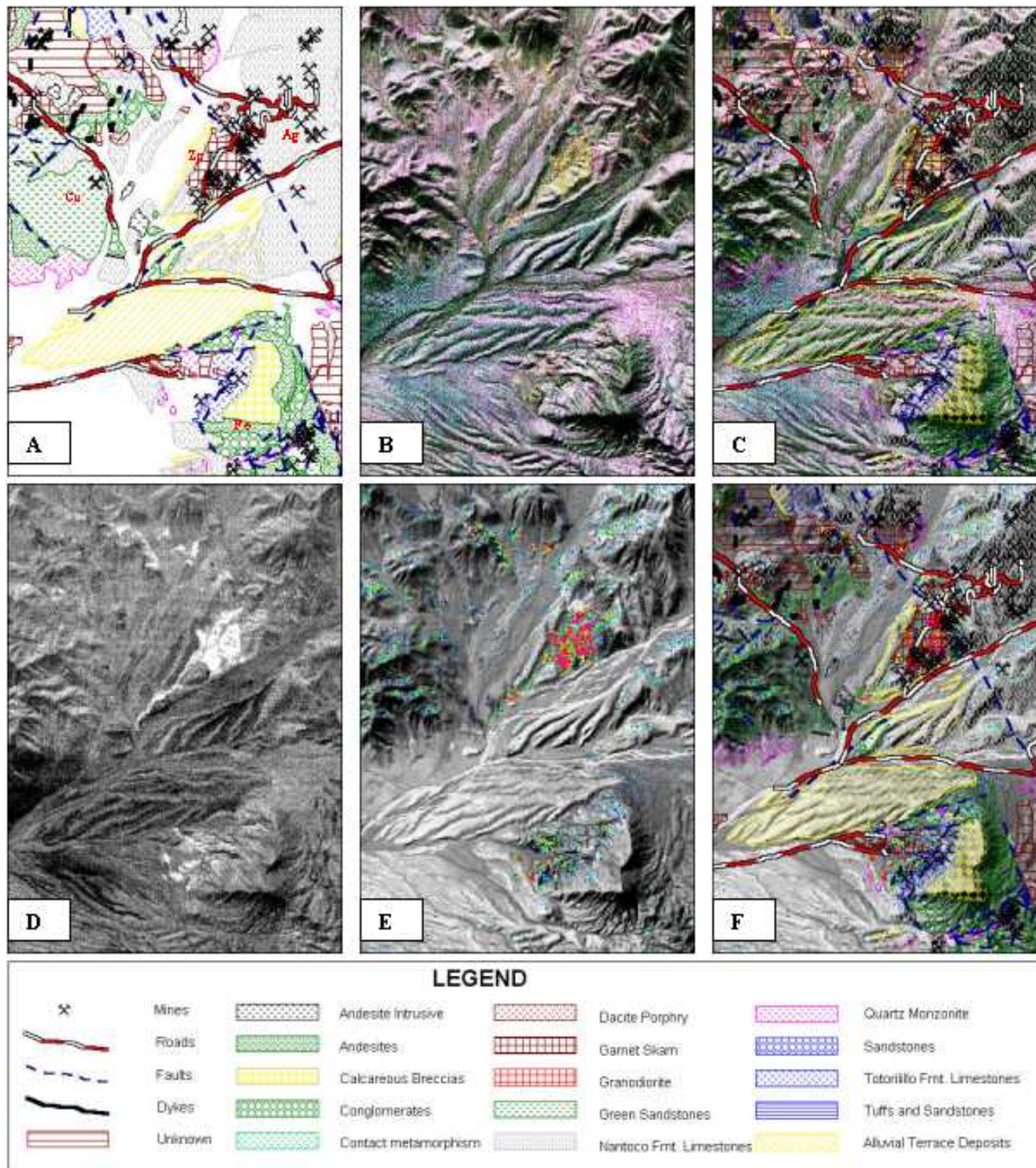


Figure 6: A) Geological map of the Chanarcillo district, N. Chile showing the location of skarn and associated silver (Ag), zinc (Zn), copper (Cu) and magnetite (Fe) mineralization. B) Geoscan MkII band 10, 11, 12 RGB image showing garnets in yellow and silica in blue. C) The same image as in B with the geology (A) superimposed. D) A simple grey-scale garnet or skarn index developed from the Geoscan MKII image data. E) The garnet or skarn index as a pseudocolour intensity index draped on a simple albedo image. F) The same image as in D with the geology superimposed. (After Pavez & Agar, 2001).

The ARGUSTM system (Hausknecht et al., 1999 & 2000) is an innovative combination of airborne hyperspectral remote sensing with airborne geophysical technologies operating simultaneously. A gamma ray spectrometer and a cesium magnetometer are operated simultaneously with three separate spectrometers; the VNIR spans 0.37 μm –1.05 μm at 0.005 μm spectral resolution; the SWIR spans 0.90–2.5 μm at 0.01 μm spectral resolution; and the TIR that spans 7.8 to 13 μm at 0.06 μm spectral resolution (Hausknecht et al., 2000). Combined, the three spectrometers provide 400 discrete spectral channels from a contiguous line profile footprint of approximately 10 meters along each flight line.

The system has demonstrated some technical successes such as the Panorama case study in Western Australia (Hausknecht et al., 2004), but has yet to become widely used. This may be due to the different roles typically played by aeromagnetic and radiometric surveys that are traditionally flown over wide areas with significant surface cover and hyperspectral data that are best applied where there is minimal surface cover and good outcrop. Furthermore, spectral profiling along widely spaced lines is not a cost-effective use of the technology and companies requiring geophysical data were not willing to pay a premium for the additional spectral data.

Ten years ago, almost all of the sensors used in or developed for mineral exploration had been whisk-broom scanning systems. Whisk-broom sensors operate using a rotating mirror to scan across a swath of ground, collecting data in a fixed angular instantaneous field of view, building up an image pixel by pixel across the flight path and line by line as the platform progresses forwards. Another type of sensor, the push-broom, collects data on a line by line basis with each pixel across the line having its own detector array.

Although the data quality of the whisk-broom systems had seen a marked improvement over time, they were still second to the push-broom type of sensor in terms of their signal:noise characteristics. In 1997, push broom sensors were limited by the size of available optical arrays and also the difficulty of calibrating and leveling each detector within the array. Bad pixels and image striping caused by inconsistencies in detector performance continue to be issues with these sensors and the data processing has required the development of new routines and software to reduce the impact of these problems.

The Canadian Centre for Remote Sensing developed sensors, the Compact Airborne Spectrographic Imager (CASI), which collected data only in the visible and near-infrared, and its short-wave equivalent, the SWIR Full Spectrum Imager (SFSI) (Neville et al., 1995), were also innovative in that they had the capacity to vary the spectral bands collected across a set range. However, although both sensors have been applied successfully to mineral exploration (Stanz et al., 1999), their overall usage has been limited due largely to their narrow swath width (2km), which increases the amount of flying involved and hence adds to the survey cost. Another limiting factor is the need to merge the two separate VNIR and SWIR sets of data and the geometric issues associated with airborne data collection.

More recent push-broom sensors such as the Spectir HyperSpecTIR (HST) and Spectir ProSpecTIR (AISA dual VNIR/SWIR) instruments have a spectral range of 450nm to 2450nm and consist of up to 499 spectral channels. The HST instrument can be operated in a ground static-horizontal

operation mode, as well as in airborne mode. The spatial resolution ranges from 0.1–3m in the static ground collections to 0.25–5m from airborne collections. These capabilities take the application to very high spectral and spatial resolution data products in regional and district scale exploration as well as mine and pit-scale mapping applications. SpecTir data applied to the Virginia City area of Nevada performed very well in comparison to other data (Hauff, 2005). Only field spectroscopy with a 5nm spectral resolution is capable of discriminating the full suite of alteration mineral suite but SpecTir was demonstrably the best of the airborne and satellite data sets, mapping three distinct types of illite plus dickite, kaolinite and alunite (Hauff, 2005).

The Hyperion hyperspectral sensor was also a push-broom type and was one of a number of instruments on the NASA EO-1 satellite that was launched in 2000 as part of a one-year technology validation and/or demonstration mission. Hyperion provides high-resolution hyperspectral imagery across 220 spectral bands in the range 0.4 to 2.5 μm with a 30-meter resolution (Figure 2). The 220 narrow spectral bands demanded that the pixel size be large in order to maintain a reasonably high signal-to-noise. Although Hyperion data evaluated over the Mt. Fitton region of Australia proved successful even with the relatively noisy data (Cudahy et al., 2001), the signal-to-noise ratio of 50:1 (Kruse et al, 2002) for the Hyperion data was generally insufficient in anything other than ideal, hyper-arid settings to discriminate individual alteration minerals. Furthermore, a 30m pixel will usually produce a mixed mineral spectrum and so signal-to-noise needs to be very good (>100:1, Kruse et al, 2002) to resolve mineral mapping at sub-pixel scales. This, coupled with the high relative cost (Table 1) plus the lack of archive data and the need to task data capture limited the use of Hyperion data in exploration. Nevertheless, the data nevertheless demonstrated that space borne hyperspectral remote sensing was technologically feasible (Cudahy et. al., 2001, Kruse et al, 2002).

On the same platform, NASA also included the Linear Etalon Imaging Spectrometer Array (LEISA) Atmospheric Corrector (LAC) (Reuter et al., 2001) which was designed to capture spectral data in the 0.85–1.5 μm wavelength range specifically for use in the optimal atmospheric correction of high spatial resolution images by using the instrument measurements of actual rather than modeled atmospheric water vapour absorption values.

From a mineral exploration perspective, the major leap forward in spaceborne remote sensing came with the launch of the Advanced Spaceborne Thermal Emission and Reflection Radiometer (ASTER) and the Moderate Resolution Imaging Spectroradiometer MODIS sensors on the Terra satellite launched by NASA in joint venture with the Japanese and Canadian aerospace agencies in November 1999 (Duda, 2004, Watanabe, 2002 & 2004).

Whereas the ASTER sensor provides multispectral data in the VNIR, SWIR and TIR (Figure 2), MODIS provides lower spatial resolution data in the VNIR and TIR that can be used to provide atmospheric water vapour information for accurate correction of the ASTER product. It was originally intended to use this for generating reflectance data as a standard product but it was never fully implemented. From a mineral exploration perspective, ASTER is important because it is the first

Table 1: Approximate data acquisition costs for selected satellite and airborne sensors.

Sensor	Scene area (sq.km.)	Cost/sq. km.	Notes
Landsat TM	32,400	\$0 to \$0.02	Geocover archive data is free but limited, other scenes cost up to \$600/scene
ASTER	3,600	\$0.02	Archival data, tasking for new data is difficult
Hyperion	315	\$7.94	Capture has to be tasked, minimum charge = \$2,500
Geoscan	Variable	\$0.50	Archival data only, assuming pixel size of 10m
Hymap	Variable	\$40.00*	Assuming pixel size of 5 m
ProSpectir	Variable	\$105.00*	Assuming pixel size of 3 m

* Airborne data costs vary significantly depending on the survey location and mobilization costs. Costs here are for data acquisition without mobilization.

spaceborne sensor to provide multi-spectral data in the SWIR and TIR parts of the spectrum, allowing discrimination of hydrothermal alteration mineralogy in the SWIR and silicate mineralogy, especially quartz, in the TIR. Furthermore, by comparison with other data, ASTER is on a par with Landsat in terms of cost (Table 1) and data is archived making it readily available.

Although ASTER data are not without problems in terms of quality, there being an issue of “crosstalk” or energy spill-over across detectors (Figure 7) (Iwasaki et al., 2001), and a consistent flaw in data caused by a fault in the diffraction grating (Figure 8) (Coulter, 2002), the data have and continue to be used successfully in regional mineral exploration having

demonstrated their capacity to map geology and accurately locate key hydrothermal alteration minerals and thus generate geologic exploration targets as opposed to spectral anomalies (Hewson et al., 2001; Rowan & Mars, 2003; Rowan et al. 2003). Another useful characteristic of ASTER data is the collection of a single backward-looking panchromatic band in the VNIR that enables the data to be used to generate digital elevation models and hence provide pseudo-stereo visualization and ortho-correction of the imagery (Toutin, 2001). This capability allows geologists to view hydrothermal alteration mineral maps derived from ASTER image data on 3-D models derived from the same data set and presented in stereo for on-screen visualization, analysis, interpretation and digitization (Figure 9).

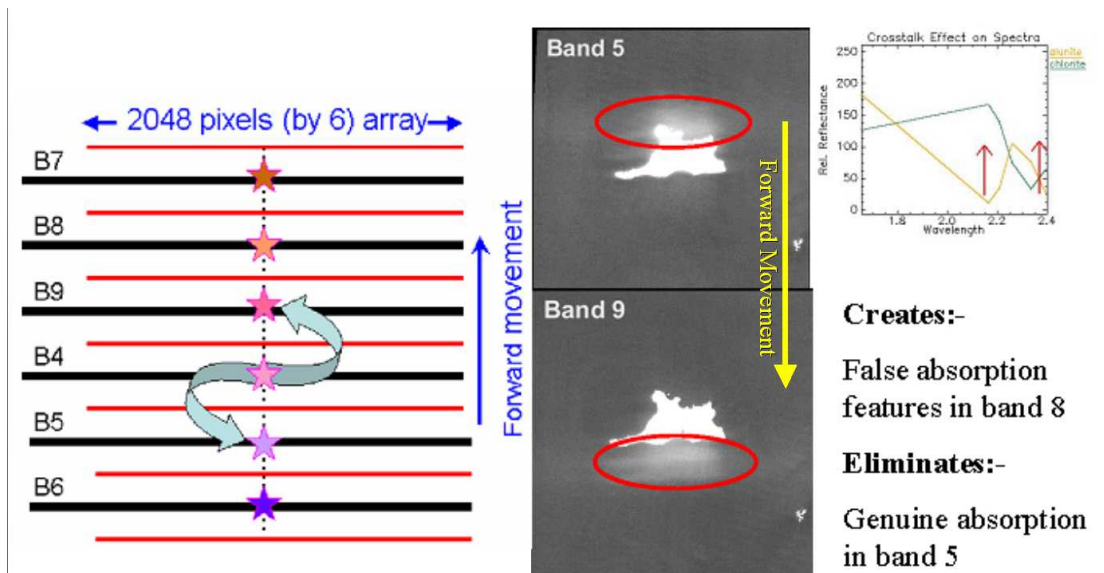


Figure 7: Schematic illustration of the “Crosstalk” problem in ASTER showing the spillover or leakage of energy from detector 4 into detectors 5 and 9 relative to the forward motion of the sensor (left), the visual impact on the image demonstrated by the “ghosting” effects in bands 5 and 9 relative to the sensor motion (centre) and the spectral effects of eliminating real absorption in band 5 and creating false absorption in bands 6 and 8 (right).

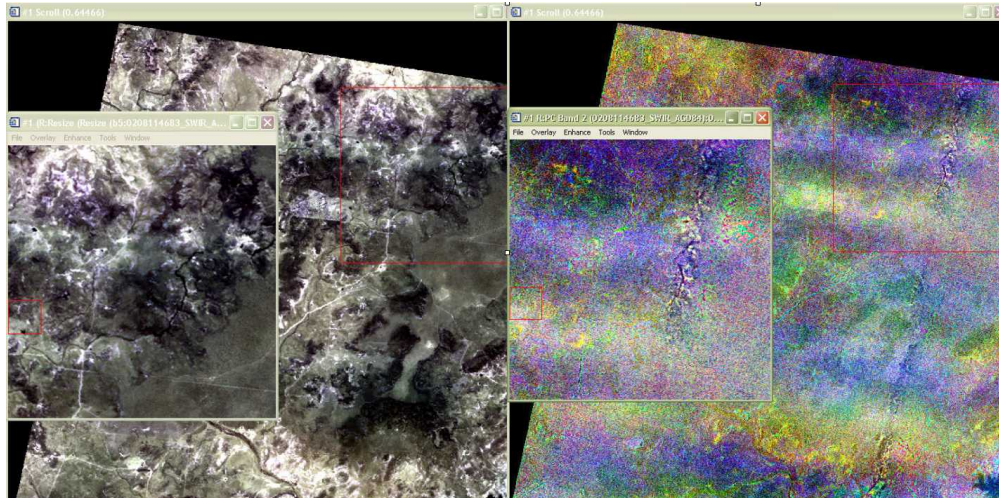


Figure 8: Simple SWIR RGB band display of ASTER image data (left) appears to be without flaws but a processed band ratio image (right) shows an orbit parallel array of noise features produced by a flaw in the ASTER diffraction grating.

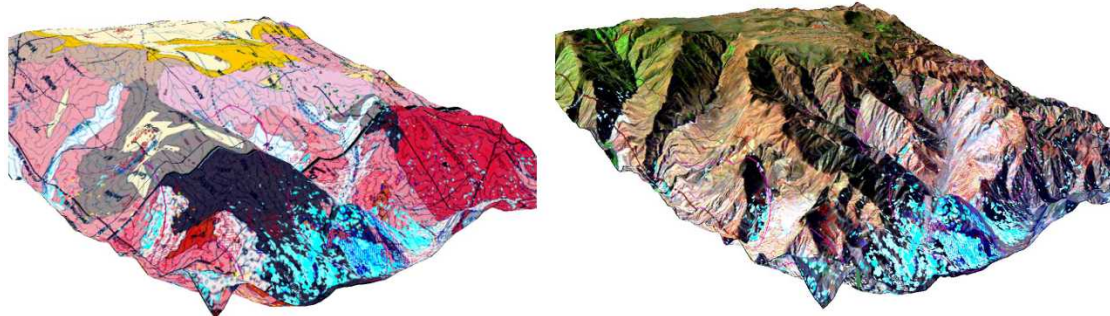


Figure 9: ASTER derived DTM used to generate 3-D visualisations of phyllic alteration (light blue) relative to mapped geology (left) and standard image algorithms (right).

Digital elevation models (DEM) have become commonplace over the last 10 years. Landsat TM-7, SPOT, ASTER, IKONOS and Quickbird imagery can all produce DEM's at various resolutions from 30 m down to 1 m and the Shuttle Radar has provided a global digital terrain model (SRTM-90) with a 90m resolution that is freely available to all users (Farr & Kobrick, 2000; Hensley et al., 2000). For detailed terrain modeling and analysis, airborne Synthetic Aperture Radar (SAR) and laser Light Detection and Ranging (LIDAR) instruments or high spatial resolution spectral instruments such as SPOT-5, Quickbird and Ikonos have the capacity to produce high quality digital elevation models and stereo-vision at finer spatial resolutions. The high spatial resolution spectral sensors SPOT-5, Quickbird and Ikonos are limited to just 4 spectral bands and are of limited use in mineral exploration other than in provision of high-resolution base image-maps for topographic and mapping work. However, with SRTM and ASTER data, the geologist now has the capacity to work with digital satellite image products in 3-D at all scales from the broad regional down to detailed prospect, project and even operational levels and to integrate the terrain data with all other digital exploration data.

Ground and field portable spectrometers

The last 10 years has not only seen major advances in sensor technology for airborne and satellite borne instruments but there have also been significant advances in ground and field portable spectroscopy that support and provide the basis for the remote sensing developments. In 1997, the Portable Infrared Mineral Analyzer (PIMA) was seeing increasing popularity as a field tool for hydrothermal alteration mapping (Thompson et al., 1999). Cabale of collecting spectral data from hand specimens, soil and rock chip samples, drill cuttings and core, the instrument was adding significant information to the understanding of alteration mineral assemblages and to the chemical variations of key alteration minerals as manifested by subtle changes in their infrared spectra (Thompson et al., 1999; Pontual, 2004).

The PIMA alone was a major factor in the development of infra-red spectroscopy as a field tool in mineral exploration and hyperspectral remote sensing as a regional alteration detection and mapping tool. The instrument covers only the SWIR wavelength range from 1300nm to 2500nm with a spectral resolution of approximately 7nm. Data capture is relatively slow, taking up to several minutes for each reading limiting the user to 200-300 readings per day (Hauff, 2004).

The Analytical Spectral Devices' (ASD) FieldSpec Pro FR spectrometer by comparison, collects data across the 350-2500nm range with a 10nm spectral resolution, integrating spectra collected every 100 milliseconds over a user determined interval to permit recording of more than 1000 readings in a day (Hauff, 2004). The FieldSpec Pro also has the capacity to be used passively with a solar energy input and to take measurements across a distance using a different fore-optic and is particularly useful for remote sensing applications where real time ground measurements can be needed in support of airborne survey data for accurate calibration purposes. The instrument was considered too expensive by most mineral industry users and the PIMA remained the most common field spectrometer until recently.

The TerraSpec, also produced by ASD, came on the market in 2004 and was designed specifically for the mineral industry. It combined all of the FieldSpec Pro FR features apart from the passive, remote sensing capability but with an enhanced spectral resolution of 5nm and a more competitive price (Hauff, 2004). The enhanced spectral resolution enables the discrimination of subtle wavelength variations in key alteration minerals, such as chlorites for example, that can be used as vectors to mineralization (Figure 10). This, coupled with the more efficient data capture has seen this instrument replace the PIMA as the preferred field spectroscopy tool and has also driven research into the development of pit-face and mine mapping instruments and core logging tools.

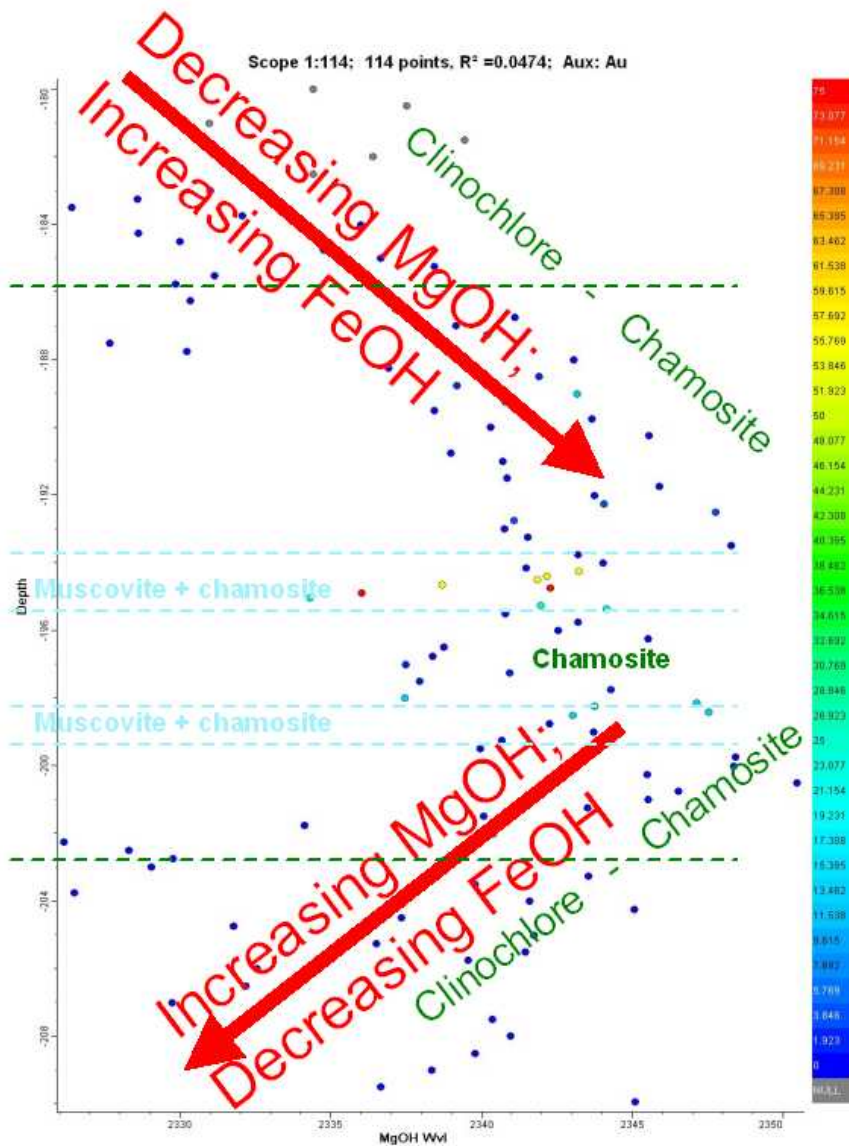


Figure 10: ASD TerraSpec analysis of drill core from the Jundee gold mine, Western Australia showing the increase in chlorite absorption wavelength and hence FeOH content relative to MgOH towards mineralization in both the hanging wall and footwall. Colour scale relates to gold grade.

The Australian CSIRO has developed both pit-mapping and core logging tools based upon ASD spectrometers with the Hy-Logger and Hy-Chips programs being offered on a semi-commercial basis (Quigley et al., 2004; Mauger et al., 2004). Both of these systems utilize ASD spectrometers coupled with 2D translation tables and robotics and can be developed for any organization with an ASD or similar spectrometer.

As mentioned above, the HyperSpecTIR suite of instruments can be operated in a ground static-horizontal operation mode and can serve the mine and pit-mapping application by producing high spatial and spectral resolution imagery rather than a series of average spectra collected at intervals as is the case with the CSIRO pit-mapping methodology (Cudahy & Ramaidou, 2004). Similarly, the SpecTerra Core Imaging system supercedes the Hy-Logger tool in that it collects hyperspectral imagery of the core at a spectral resolution of 3 nm and a spatial resolution of 0.5 mm, taking infrared reflectance spectroscopy almost into the realm of petrography (Figure 11) (Linton et al., 2004; Harris et al., 2006).

The last 10 years have therefore seen remote sensing instruments improve in terms of their spatial and spectral resolutions through the development of better sensor technologies. Signal-to-noise characteristics have been improved so that subtle variations in mineral chemistry can now be mapped remotely. The spatial accuracy of remotely sensed data has benefited from GPS technologies and the development of digital Terrain Models from radar, lidar and spectral instruments at all scales from the regional using SRTM and/or ASTER data to project levels using Quickbird, Ikonos or Lidar for example. Developments in field spectroscopy have helped drive the improvements in remote sensing instruments which have in turn contributed to detailed spectroscopic analysis of pit

and mine faces as well as drill core, so that spectral remote sensing now encompasses all scales from regional alteration mapping down to petrographic analysis of drill core

Data Analysis in the 21st Century – the Spectroscopic Revolution

The correction and analysis of remote sensing data are the critical steps that convert the data into useful information. The ultimate goal is the generation of mineral maps – either as the dominant mineral or the mixture of minerals in each image pixel. The recent advances in data analysis have focused on data inversion using spectroscopic processing. This primarily involves the application of statistical and signal processing methods in a way that the entire spectrum is analyzed. This section provides an overview of currently used, common processing methods. No attempt is made to provide a comparison of software packages, instead algorithms are explained both qualitatively and mathematically.

The analysis of remote sensing data has often been undertaken as a qualitative interpretation exercise. Processing often consists of the generation of derivative processed imagery and directly visualized. Part of the motivation for this is the acuity of human vision. Our ability to see subtleties of colour and texture is highly developed but the ability to quantify these characteristics is not. As higher spectral resolution data has become available, there has been a commensurate need need for more quantitative approaches to data analysis. Spectral processing methods allow remote sensing data to be semi-quantitatively or quantitatively inverted to physical mineral metrics that directly relate to ore forming processes.

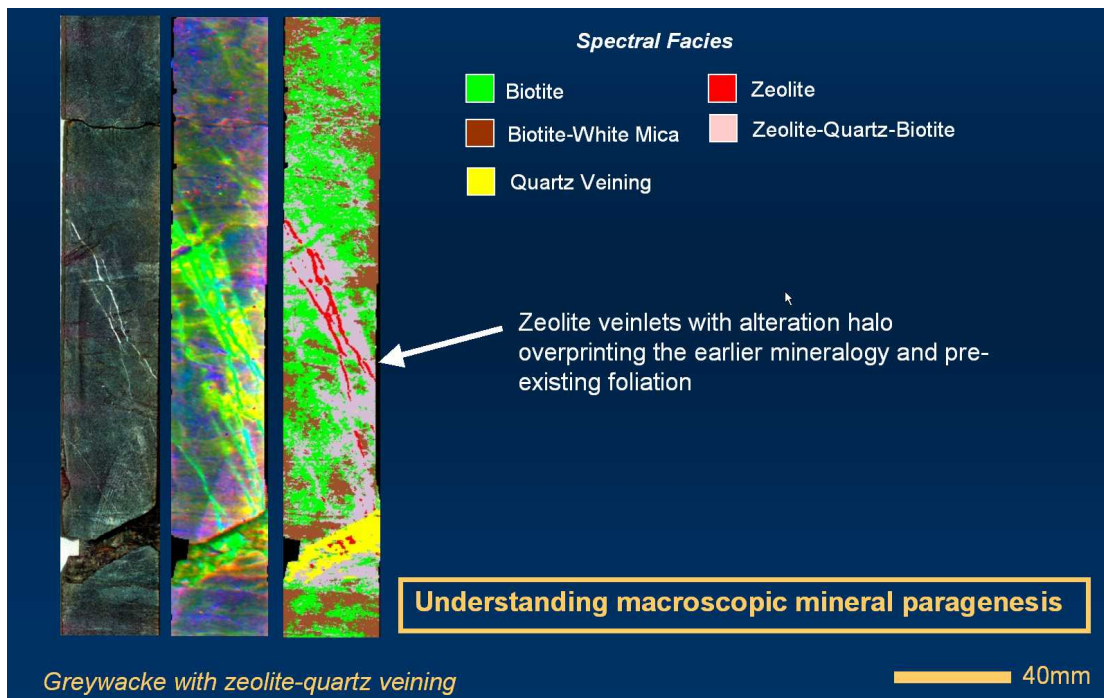


Figure 11: The use of hyperspectral core scanning to understand alteration paragenesis demonstrated in an example using the SpecTerra Core Imaging System operated by Anglo-American (after Harris et al., 2006).

Calibration and Atmospheric Correction

A critical limitation on remote sensing data in the past was the lack of reliable methods for data calibration. Calibration is the removal of the effects of atmospheric interference on the reflected signal received at the sensor. The calibration process results in measurements that appear as similar as possible to laboratory or field reflectance data. This allows a direct comparison to be made between the image spectra and known mineral spectra. The calibration step, although sometimes time consuming, makes the data analysis much easier and more reliable. In many cases we need to match the results of analyses from images acquired on different dates (e.g., when mosaicing scenes) or compare results from different areas. Careful calibration allows these actions to be carried out relatively easily.

All earth remote sensing data are collected through the earth's atmosphere as radiance at sensor measurements. Multispectral images are typically collected in atmospheric windows where in little of the energy is absorbed by the atmosphere. Scattered energy, however, is collected by the

sensor and some atmospheric absorption is always present. Hyperspectral images are collected across all wavelengths and contain the atmospheric absorptions and scattering. Scattering and absorption are wavelength (band) dependent (Figure 12). Scattering is primarily due to atmospheric gases (Rayleigh scattering) and particulates (Mie scattering) (Schowengerdt, 1997). Absorption is primarily due to carbon dioxide, water vapor, and ozone. Of these variables, water vapor and particulates have the greatest spatial and temporal variability in concentration. If a pure uniform atmosphere was assumed, the effects could easily be removed, in practice, a custom correction for each image based on local atmospheric conditions is required. The atmospheric contributions need to be removed so that the image band responses match the reflectance response of the material on the earth's surface. It is important to note that there are other physical and optical parameters that are ignored here, thus we refer to the results of atmospheric correction as "apparent reflectance".

A number of approaches may be used to calibrate image data to apparent reflectance (Table 2). Calibration methods may be based on an atmospheric model, data derived, or based on the known spectrum of the ground.

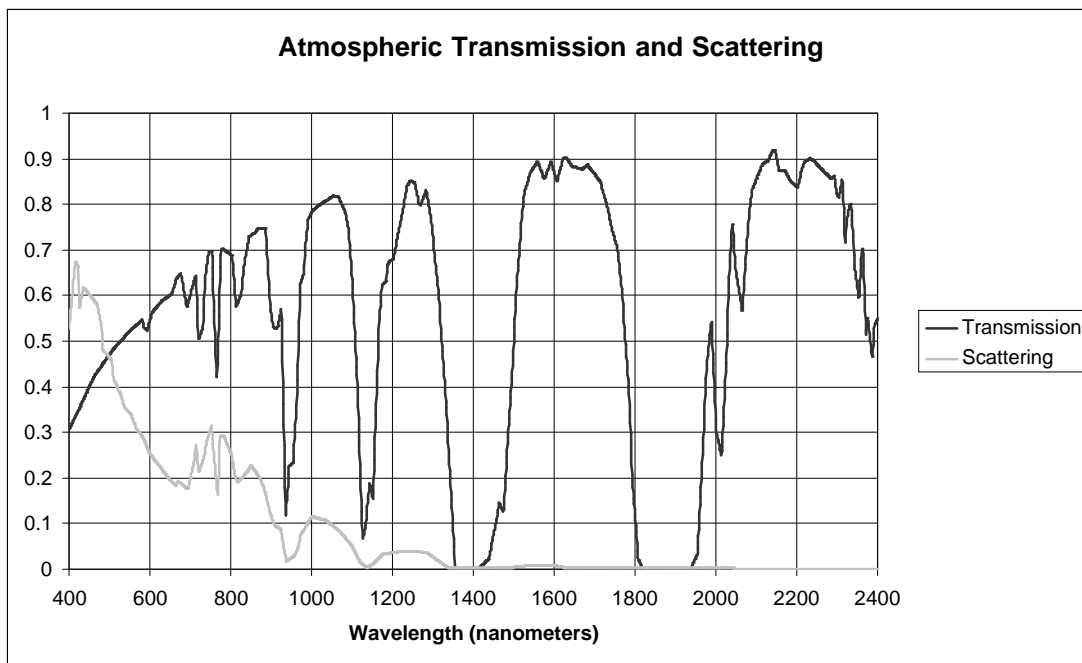


Figure 12: Atmospheric transmission and scattering.

Table 2: Summary of calibration methods.

Calibration Method	Comments
Internal Average Relative Reflectance	Requires a large image (e.g., TM full scene) and minimal vegetation
Log Residual	Removes topographic shading
Model Based	Typically requires multiple iterations to get correct parameters
Flat Field	May require field work to identify an acceptable flat field
Empirical Line	Always requires field work and the availability of a field spectrometer

Atmospheric model based calibration methods include MODerate spectral resolution atmospheric TRANSmittance (MODTRAN), Fast Line-of-sight Atmospheric Analysis of Spectral Hypercubes (FLAASH), ATmosphere REMoval program (ATREM), Atmospheric CORrection Now (ACORN), and High-accuracy Atmospheric Correction for Hyperspectral data (HATCH). All of the model based corrections require knowledge of the location, altitude, date, and time of image acquisition. When correcting hyperspectral data the local atmospheric conditions (primarily water vapor content of the atmosphere) may be estimated from the data as the atmospheric absorptions are measured. For multispectral data, an estimate of the local atmospheric conditions must be made or derived from an external data set (a concurrent MODIS image for example in the case of ASTER data). The use of model based calibration is almost always an iterative process that requires the “tweaking” of parameters to get an acceptable result.

Data derived calibration is often the quickest and easiest method to achieve an acceptable result. The Internal Average Relative Reflectance (IARR) method simply normalizes an image by the average spectrum of the entire scene which is assumed to be dominated by the atmospheric signature. This method works well in un-vegetated areas (RSI, 2005). Also, larger images tend to produce better results. Thus IARR works better on a TM image than an ASTER image. The Log Residual method was developed for airborne imagery (Green and Craig, 1985) and involves normalization by an albedo image. This is calculated as a geometric average rather than a mathematical average.

The Flat Field calibration method requires that a “spectrally flat” area on the ground be identified. This may be done in the field or on the basis of geologic knowledge. Clean sandstones, quartzite, (quartz) dune sand, or (quartz) beach sand typically have spectrally flat responses. A transformation is calculated that flattens the observed spectra of the flat field. This transformation is applied to all pixels in the image.

A related calibration is the Empirical Line method. In this approach an area is identified on the ground and the spectral response is measure with a field spectrometer. A transformation is then calculated that forces the image spectra to match the field spectra and is applied to the entire image.

These methods are typically applied individually. In some cases a model based calibration may be used to get a first approximation and then the empirical line method applied as a refinement (Clark et al., 2002).

Spectral Processing Methods

Once an image is calibrated, regardless of whether it is multispectral or hyperspectral, a wide variety of spectral processing tools may be applied to it. The commonly used spectral analysis methods fall into two broad categories: classification methods and unmixing methods. Classification methods attempt to assign each pixel in an image to a class that, in the case of geologic problems, are minerals or materials of interest. Unmixing methods, on the other hand, attempt to assign a concentration for each mineral of interest to each pixel. In both types of analysis a confidence image may be calculated

to provide an indication of the accuracy of the classification or unmixing. In geophysical terms, all of these methods are inversions of the remote sensing data. The data are inverted to a binary map (each pixel is all of a single mineral) or a scaled map (each pixel has a mixture of minerals).

Preprocessing – Endmember Identification and Feature Selection

The identification of mineral endmembers in multispectral or hyperspectral data is the starting point for data analysis. An endmember may be a pure mineral spectrum or a mixture of spectra of materials of interest. Endmembers may be identified through automated or manual data mining techniques, by direct measurements taken in the field, or a combination of these techniques. Regardless of which approach to endmember selection is undertaken, it is generally considered best to use spectra extracted from the image data as endmembers for further data analysis. Image derived endmembers are viewed as being superior to spectral library or laboratory endmembers because they contain any residual atmospheric and instrumental characteristics (van der Meer 2000).

A common data mining method used for endmember identification is described in Boardman et al. (1995) and has been given the name Pixel Purity Index (PPI). This is implemented in the ENVI software package. The PPI method involves iterative identification of image pixels that are outliers within the multidimensional data vector space. “The Pixel Purity Index is computed by repeatedly projecting n-dimensional scatterplots onto a random unit vector. The extreme pixels in each projection-those pixels that fall onto the ends of the unit vector-are recorded and the total number of times each pixel is marked as extreme is noted.” (RSI 2005) Although the technique identifies “mathematically” good endmembers, it is unconstrained by any a priori knowledge of the field occurrences of minerals or minerals that are of interest in the study.

A second school of thought on endmember selection is based on building a large body of a priori knowledge of the field mineral occurrences. This approach involves the development and/or research of geologic models for the studied systems, manual data mining of the spectral response of image pixels, and collection and spectroscopic analysis of field samples. The approach does not lend itself to a rote sequence of activities, but follows an iterative paradigm of building a knowledge base of endmember minerals through a number of activities. The easiest (and cheapest) activity is a review of the literature to get a basic understanding of the geologic systems in the study area. From this, general ideas may be developed about the types of minerals that will be found in the field. If imagery data have already been acquired, it is often useful to manually inspect the spectra of image pixels. This activity, a “virtual field trip”, helps to determine if the image spectroscopy makes sense in light of the geologic model and provides some guidance for field work. Direct field inspection of the ground is the most critical aspect of endmember selection. Sample locations are visited based on the literature, the preliminary image analysis, and geologic experience. The sampled materials are subjected to field or laboratory spectroscopic analysis to determine the suite of minerals that is present and important to the study. These activities are repeated and may continue through-out the study as

the detailed geologic model evolves. In most cases, however, the most abundant and important endmember minerals are quickly identified.

Classification

Classification methods assign each pixel in an image to a group or class based on similarity criteria. Classifications may be hard or soft. Hard classifications assign a single class to each pixel whereas soft classifications assign a similarity metric to each pixel for each class (Schowengerdt 1997). A soft classification may also be called a “rule image”.

A number of classification methods are commonly used for geologic remote sensing. These are: Spectral Feature Fitting (SFF), Spectral Angle Mapper (SAM), and Spectral Correlation Mapper (SCM). Each of these approaches has benefits and limitations and is briefly described below.

Spectral Feature Fitting is used by the USGS and also implemented in the ENVI package. The USGS calls their version of SFF “Tetracorder” which is described in Clark (1990) and Clark et al. (1999). Tetracorder includes some expert-system heuristics in addition to the basic SFF methodology. The SFF method involves analysis of each spectral absorption feature and comparison of these against absorption features in endmember spectra. Each feature is extracted from the image spectrum and endmember spectra (the endmember spectra are resampled to the image spectra resolution if needed). The absorption features are subjected to a continuum removal (hull correction) and the depth and shape of the image and endmember features are compared. The result of the analysis is a feature depth metric and a goodness-of-fit which are typically combined to produce a soft classification image (Farrand, 2001).

Spectral Angle Mapper was first described in Kruse et al. (1993) and was implemented within the Spectral Image Processing System (SIPS) software package. SAM is a simple vector space calculation that provides a similarity metric between each image pixel spectrum and endmember spectra. In geometric terms, SAM is the angle between the image spectrum vector and the endmember spectrum vector. It is defined mathematically as follows (Modified from Carvalho and Meneses, 2000):

$$S = \cos^{-1} \frac{\sum_{i=1}^n X_i U_i}{\sqrt{\sum_{i=1}^n X_i^2 \sum_{i=1}^n U_i^2}}$$

Where:

- S is the spectral angle
- X is the endmember spectrum
- U is the unknown (image) spectrum

The SAM calculation results in a value of zero for good matches between the image spectrum and the endmember spectrum.

It was noted by Carvalho and Meneses (2000) that SAM is actually a variant of the more general Pearson Correlation

Coefficient and that the SAM approach is actually a “folded” version of the correlation coefficient. The result is that perfect mirror images between the image and endmember spectrum also produce a SAM angle of zero. This is an unlikely situation in hyperspectral data but is common in multispectral data such as ASTER or TM. They propose use of the correlation coefficient as a better classification than SAM and call the method the Spectral Correlation Mapper (SCM). Landgrebe (2003) refers to this as simply the Correlation Classifier (CC).

Classification using a correlation approach has a distinct advantage in that it provides a direct measurement of the similarity between the shapes of two spectra. Furthermore, Carvalho and Meneses (2000) show that the SCM calculation is relatively immune to amplitude differences between the image and endmember spectra making the method relatively robust under different image shadow conditions. The SCM method is defined mathematically as follows (Modified from Carvalho and Meneses 2000):

$$R = \frac{\sum_{i=1}^n [(X_i - \bar{X})(U_i - \bar{U})]}{\sqrt{\sum_{i=1}^n (X_i - \bar{X})^2 \sum_{i=1}^n (U_i - \bar{U})^2}}$$

Where:

- R is the correlation coefficient
- X is the endmember spectrum
- \bar{X} is the mean of the endmember spectrum
- U is the unknown (image) spectrum
- \bar{U} is the mean of the unknown (image) spectrum

This results in a correlation coefficient image in which each pixel is assigned a value between -1.0 and 1.0 for each endmember mineral spectrum. A value of 1.0 denotes an exact match between the endmember spectrum shape and the image spectrum shape whereas a value of -1.0 is an exact inverse match.

Unmixing

In most geologic settings, imaging remote sensing instruments measure a mixture of earth materials. Unmixing of the component mineral spectral signatures is particularly valuable in that it allows the relative concentrations of minerals to be mapped. Figure 13 illustrates the unmixing of iron minerals jarosite, goethite, and hematite in a developing leach cap over a porphyry system. The jarosite/goethite ratio is also shown in Figure 13 which highlights the location of the most intense mineralization (Anderson, 1982) and sources of natural acid drainage (Coulter, 2006). The nature of the mixture is critical for determining how the unmixing model is developed. Intimate mixtures occur at the grain size level while areal mixtures occur at a large scale and represent patches of differing material within a single pixel (Hapke 1993). It has been shown by Clark (1983) and Hapke (1993) that the spectra of intimate

mixtures are nonlinear with respect to relative concentrations. Although the non-linear behavior may be modeled analytically, a number of optical and geometric parameters are needed, making the method very cumbersome (Hapke 1993). Empirical models may also be developed but this requires some a priori knowledge of the materials in the mixtures and time consuming construction of many different mixtures in the laboratory. Because of the complexity of utilizing non-linear mixing models, remote sensing scientists rely almost exclusively on linear mixing models. In the linear model we assume that the image spectrum is the concentration weighted sum of the component spectra. That is:

$$I = \sum_{i=1}^n W_i S_i$$

Where:

- I is the image spectrum
- W_i is the i th weight
- S_i is the i th component spectrum

Full linear unmixing is often a difficult problem to solve particularly if pure mineral spectra are the desired endmembers. Full unmixing requires that all of the endmembers in an image be identified and that the total number of endmembers must be less than the total number of bands (RSI 2005; Farrand 2001). Full unmixing is normally implemented as an inversion of the mixing matrix problem. The method described by Boardman (1989) that uses Singular Value Decomposition (SVD) is a common implementation. Full unmixing is usually subject to "physical" mixing constraints: all weights must be between zero and one; and the weights must sum to one. The assumption that all image endmembers are known makes the use of full unmixing unwieldy to apply when pure mineral endmembers are desired. The inversion works well when mathematical endmembers are derived from the image data. Unfortunately, these derived endmembers may actually represent mixtures themselves and not pure mineral spectra. Partial unmixing methods are used when a selected but incomplete set of endmembers are used.

Partial unmixing methods allow a subset of the image endmembers to be used to solve the unmixing problem. The desired endmember spectra are unmixed from a "background" spectrum that can be modeled as noise (Farrand 2001). Since the goal is to enhance the desired endmember spectra and suppress the background "noise" an approach that maximizes signal to noise (SNR) is typically used to solve the problem.

The Match Filter (MF) used in signal processing is designed to solve this type of problem and is basis for most partial unmixing in remote sensing (Farrand 2001). The Match Filter algorithm is almost identical to the Constrained Energy Minimization (CEM) algorithm discussed in Farrand and Harsanyi (1997), van der Meer (2000), and Farrand (2001). The approach is to find a vector operator that suppresses the background spectrum and enhances the endmember spectrum.

The operator is constrained to have minimum energy across all pixels and have an output of 1.0 for the endmember spectrum (Farrand 2001; van der Meer 2000). Farrand (2001) defines a solution as:

$$X = \frac{[\rho]^{-1}[d]}{[d]^T[\rho]^{-1}[d]}$$

Where:

- X is the operator
- ρ is the full image correlation matrix
- d is the endmember spectrum

The operator X is applied for each endmember producing an image of endmember weights or proportions. It is important to note that the correlation matrix is nearly always singular for hyperspectral data. This requires that an approximation be used (Farrand 2001). Although the technique is simple and rapid, it may in some cases produce false positive results (RSI 2005).

In order to deal with the ill-conditioned correlation matrix and false positive problems inherent in the CEM/MF method, a technique of partial unmixing was developed by Boardman et al. (1995). This has come to be known as Mixture Tuned Match Filtering (MTMFtm).

Mixture Tuned Match Filtering (MTMFtm) is a partial unmixing method that is used extensively for mineral exploration remote sensing (Farrand 2001). It was developed by Boardman et al. (1995) and involves a number of processing steps. Prior to processing, the image data are assumed to be calibrated to apparent reflectance. The first step is a vector space rotation using the Minimum Noise Fraction (MNF) method. This method, developed by Green et al. (1988), is a principal-component-like orthogonalization rotation that results in components ordered in increasing rank of random noise rather than decreasing rank of variance. In practice, a subset of components is selected that contains most of the image information and minimum noise; the higher order (i.e., noisier) MNF components are pruned from the data. It is important to note the method assumes a random noise model and does not work on images containing coherent or periodic noise. The MNF rotation and pruning solves two critical problems with hyperspectral data: it reduces dimensionality and it results in well-conditioned (non-singular) covariance and correlation matrices. After pruning, mineral endmembers may be found using the PPI method or predetermined endmembers may be used. If predetermined endmembers are utilized from the original image data or a spectral library, their spectra must be subjected to the same MNF rotation and pruning as the image data. The CEM/MF method is then applied to the image using the transformed endmembers in MNF space. The MTMFtm calculation produces concentration and an "infeasibility" image for each endmember component image. The infeasibility image is used to threshold out any false positive results produced by the CEM/MF technique.

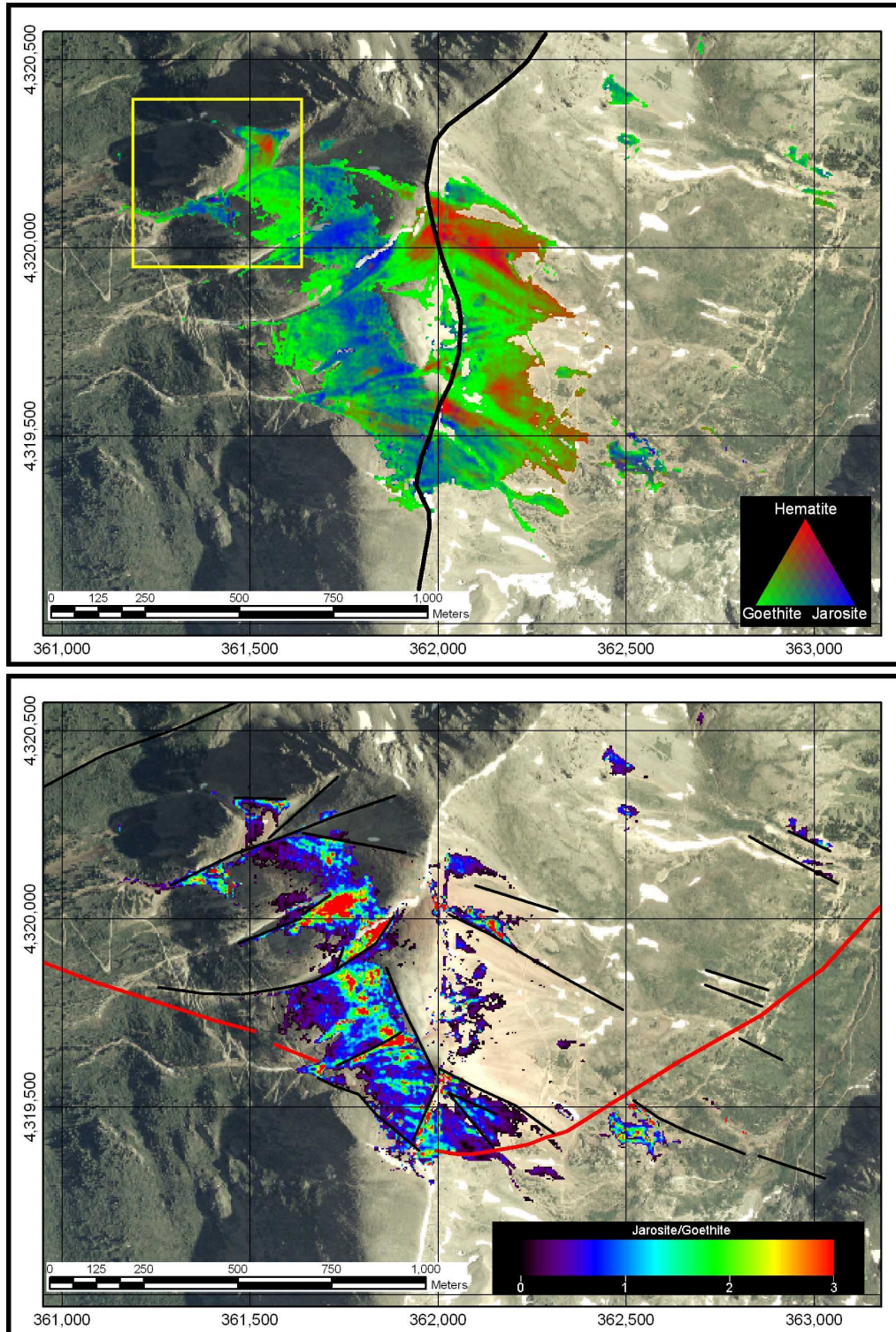


Figure 13: Partial unmixing results for iron minerals from hyperspectral data in the Grizzly Peak Caldera. The image is of a developing leach cap over an unexploited Mo-Cu porphyry. The top image maps hematite, goethite, and jarosite as RGB. The bottom image is the jarosite/goethite ratio calculated from the partial unmixing image.

New methods

It is appropriate to briefly discuss methods of analysis that are new and not yet widely used for remote sensing. Two methods are highlighted: Support Vector Machine (SVM) classification and Optimized Cross Correlation Mixture (OCCM) analysis partial unmixing.

Support Vector Machine Classification

Support Vector Machine classification has received a lot of attention for remote sensing problems in the last several years. The method allows non-linear separation of complicated, often overlapping, distributions in the image vector space (Figure 14). The goal of SVM classification is to identify a mapping of the data, through a “kernel function”, that transforms a non-linear separator into a linear separator called a hyperplane. In a simple case of a two band image, this hyperplane is a line (Figure 14) and in a three band image, a plane. In higher dimension imagery we can only define the hyperplane mathematically. An important concept of the SVM method is that it operates in the dot-product (inner product) space rather than the raw vector space. This has an interesting relationship to the SAM classification method. If we inspect the SAM equation, we see that the numerator is actually the dot product between an endmember and an image pixel. As we have seen, when normalized this provides a measure of the similarity between the

multispectral or hyperspectral signatures. Operating in dot product space has appeal as the values are a geometric measure of pixel similarities between image (unknown) pixels and some set of endmember training pixels (Chen et al., 2003). The SVM method differs from SAM in that rather than generating classification or rule images we use the distribution of the differences between the endmember pixels (as measured by the dot product of the training pixels) to generate a kernel function that allows the linear separation (or partitioning) of the entire vector space. This partitioning may then be applied to all the pixels in the image to produce a classification. Furthermore, as we are working with simple hyperplane geometry, we can also easily calculate the distance to the partitioning hyperplanes and produce a measure of the quality of the classification (Figure 15).

The primary problematic aspect of applying the SVM method to geologic problems is the scarcity of training data that are necessary for generating the partitioning hyperplanes. A reasonable sample of the population for each endmember is needed for the SVM method to produce reliable partitions of the feature space. This is often an impossible (or at best a prohibitively expensive) task that requires the collection and analysis of large numbers of ground samples. An alternative is to utilize existing spectral libraries such as the USGS library or Specmin to provide the training data.

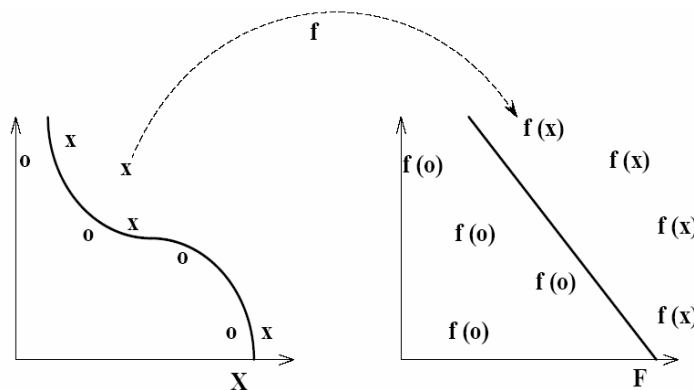


Figure 14: The SVM concept. The transformation (via a kernel function) of non-linearly separable data may allow linear separation (from Christianini, 2001).

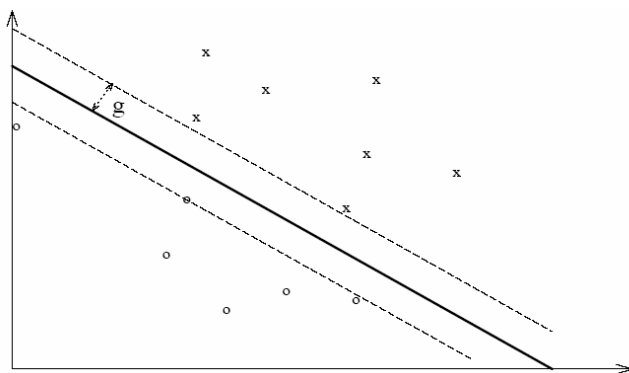


Figure 15: A quality measurement for SVM classification. The simple geometry of the SVM hyperplane (in this case a line) allows the distance to the partition to be easily calculated. In this example one might say that points that fall within distance g from the partition could belong to either class “x” or “o”.

Optimized Cross Correlation Mixture Analysis

A new partial unmixing method called Optimized Cross Correlation Mixture (OCCM) analysis is discussed in Coulter (2006). The approach is relatively immune to illumination variations and does not require re-projection of the feature space (which is important when utilizing data containing coherent noise, e.g. data from pushbroom detectors). OCCM is an extension of the Tetracorder (Clarke, et al., 1999) and SCM (Carvalho and Meneses, 2000) methods. The basic philosophy is to match the entire shape of each image pixel spectra to a linear synthetic mixture of endmember spectra. This extends feature fitting approaches in that emission maxima are modeled as well as absorption features. The method is implemented as a constrained optimization problem.

In the OCCM method the maximum cross-correlation is determined between the image spectrum and linearly mixed spectra of the endmembers of interest for each pixel. The philosophy behind the approach is that, for an image pixel spectrum to be considered a “good fit” to a target mixture spectrum, the image spectrum must closely match the shape of the spectrum of the target mixture. Thus, the cross-correlation between the image pixel spectrum and the target mixture spectrum must be close to one.

The method is defined as follows:

Find the vector of weights [W] that maximizes:

$$R = \frac{\sum_{i=1}^n [(W][E] - \overline{[W][E]})(U_i - \overline{U})]}{\sqrt{\sum_{i=1}^n ([W][E] - \overline{[W][E]})^2 \sum_{i=1}^n (U_i - \overline{U})^2}}$$

Where:

R is the correlation coefficient

$[W]$ is the weight vector

$[E]$ is the endmember spectra matrix

$\overline{[W][E]}$ is the mean of the synthetic (mixed) spectra

U is the unknown (image) spectrum

\overline{U} is the mean of the unknown (image) spectrum

n is the number of channels in the spectrum

Subject to:

$$W_i \geq 0 \text{ and } \sum W_i = 1 \text{ for all } i$$

This optimization finds the weighting factors for the endmember spectra that produce the highest cross correlation between the resulting mixture spectrum and the unknown image spectrum. Each weighting factor is constrained to be between zero and one and the sum of all the weighting factors is constrained to be less than or equal to one. The optimization identifies the mixture spectrum that most closely matches the shape of the image spectrum. An example of the objective function for a single image pixel is shown in Figure 16. Since the correlation coefficient between the best fit mixture spectrum and the image spectrum is calculated, it may be preserved and used as a threshold to reject poorly fitting results. These rejected pixels are equivalent to the partial unmixing background pixels in other partial unmixing algorithms.

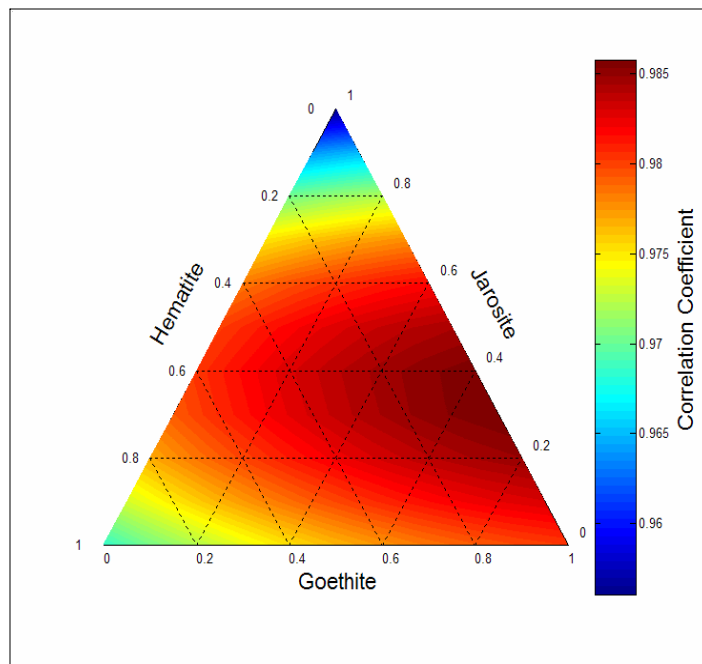


Figure 16: Objective function for partial unmixing of iron minerals. The correlation maximum is at approximately 35% jarosite and 65% goethite. This illustrates that the function is smooth and well behaved producing a fast and reliable optimization.

Examples

This section provides examples of remote sensing results from a variety of sensors and processing methods over the Goldfield and Cuprite hydrothermal systems in Nevada (Figure 17). These examples illustrate how improvements in spectral and spatial resolution and processing contribute to refinements in the alteration mapping.

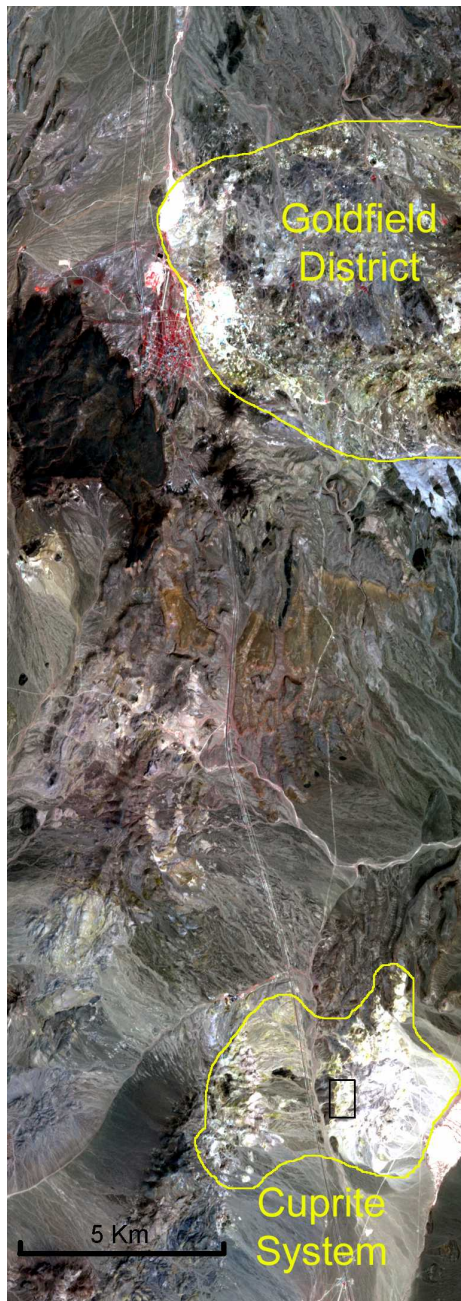


Figure 17: Overview of the Goldfield and Cuprite alteration systems. The inset box is the location of the “Buddingtonite Bump”

The Goldfield system was mined for precious metals (primarily gold) in the early 1900’s and exploration in the district continues today. The alteration is high sulfidation and is dominated by quartz-alunite ledges. Illite, kaolinite, dickite, and pyrophyllite also occur in the district. Cuprite is a largely barren hydrothermal system. It is zoned and dominated by alunite and kaolinite with a well defined silica core in the eastern part of the system. An outcrop of buddingtonite (ammoniated orthoclase) which was originally identified by remote sensing occurs in the system. Both systems have been studied extensively with remote sensing techniques.

Figure 18 shows Thematic Mapper color ratio composite and Figure 19 the TM Crosta analysis results for the study area. In both images red is mapped as “clay” (more accurately the presence of OH- anions), green is mapped as iron oxides, and blue maps vegetation. The TM imagery identifies the location of the alteration systems and clay and iron oxide zoning of the alteration. With TM we can make a qualitative statement that there are very likely alteration systems present at Goldfield and Cuprite.

Figures 20 and 21 show mineral family mapping from ASTER data undertaken with the SCM method. Figure 20 shows alunite, kaolinite, and illite mapped as RGB and Figure 21 shows iron oxides, clays, and quartz mapped as RGB. The ASTER imagery provides more highly refined mineral mapping than TM. Zoning within the alteration systems is highlighted. A unique aspect of ASTER is the multispectral thermal infrared channels. This capability allows quartz to be mapped directly and targets the most highly prospective parts of the systems. The image shown in Figure 21 is particularly useful for prospecting as it integrates iron oxide, clays (kaolinite and illite), and silica.

Figure 22 and 23 show mineral mapping from low spatial resolution AVIRIS data undertaken with partial unmixing. Figure 22 maps the dominant minerals alunite, kaolinite, and illite as RGB and Figure 23 maps the less common minerals pyrophyllite, dickite, and buddingtonite as RGB. Although there are many similarities to ASTER (which speaks well of the capabilities of ASTER), the AVIRIS results are more accurate than ASTER. AVIRIS has also mapped subtle clays in the alluvium that are not well characterized in ASTER. More importantly, AVIRIS is mapping pyrophyllite, dickite, and buddingtonite which are ambiguous at ASTER spectral resolution. These minerals indicate higher temperature parts of the system and are the locations of possible feeder structures. Unfortunately, AVIRIS does not have thermal infrared capability so quartz can not be mapped directly.

The final example is high spatial resolution (1 meter) hyperspectral data from the Spectir/AISA “Dual” airborne system. These images cover the “Buddingtonite Bump” area at Cuprite (Figure 17, inset box). Figure 24 is partial unmixing results showing alunite, kaolinite, and illite. Figure 25 is the partial unmixing results showing alunite, kaolinite, and buddingtonite. These results illustrate the advantage of high spectral resolution hyperspectral imagery for mapping alteration minerals at the outcrop scale.

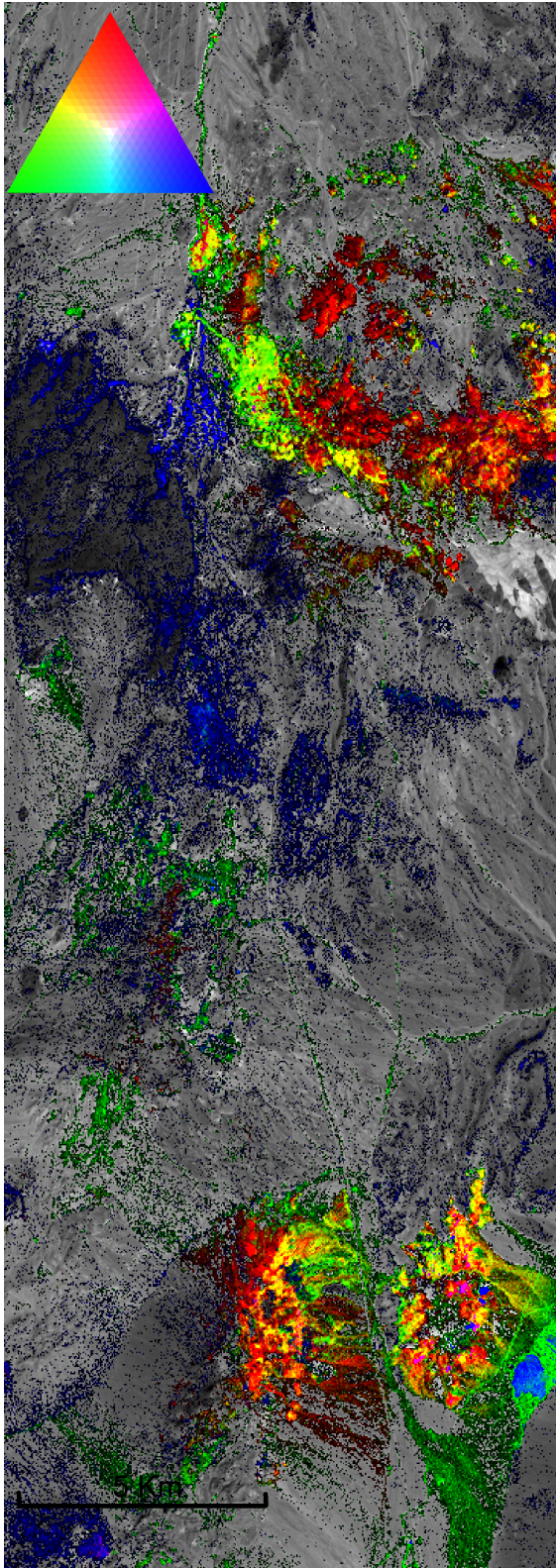


Figure 18: Color ratio composite of TM imagery over Goldfield and Cuprite areas in Nevada. RGB are mapped as OH (clay), Iron Oxide, and vegetation/non-altered.

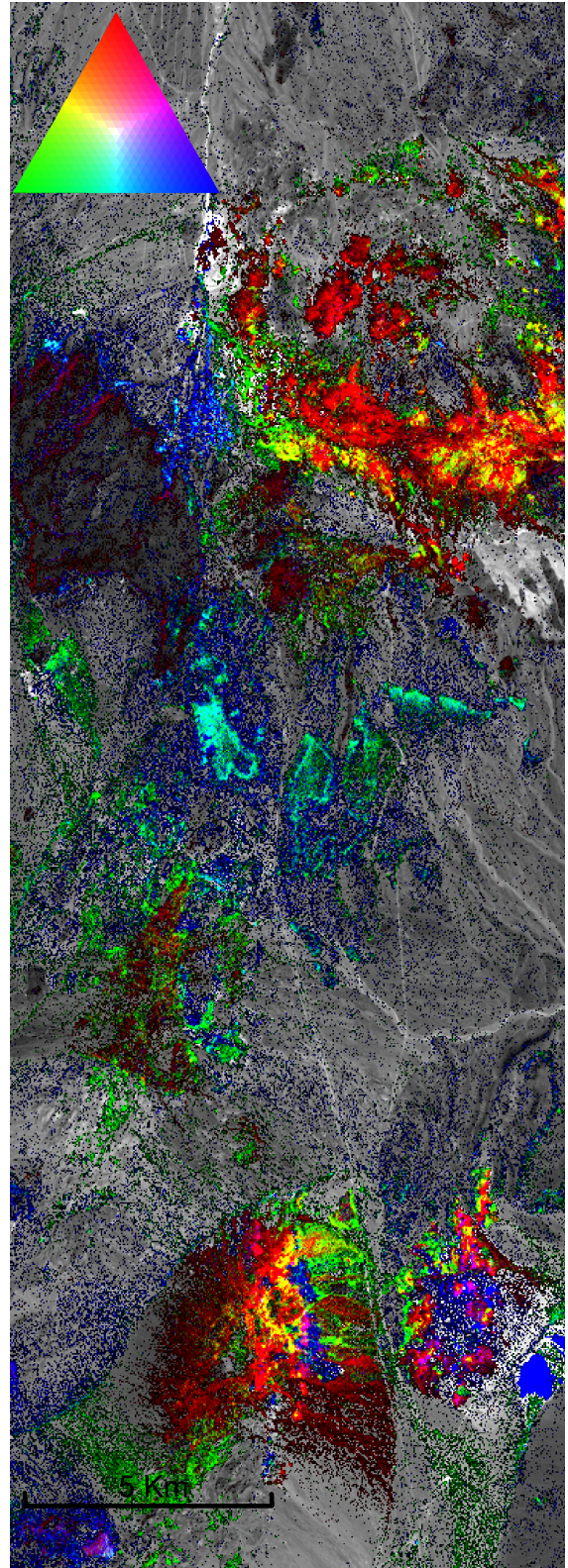


Figure 19: Crosta analysis of TM imagery over Goldfield and Cuprite areas in Nevada. RGB are mapped as OH (clay), Iron Oxide, and vegetation/non-altered.

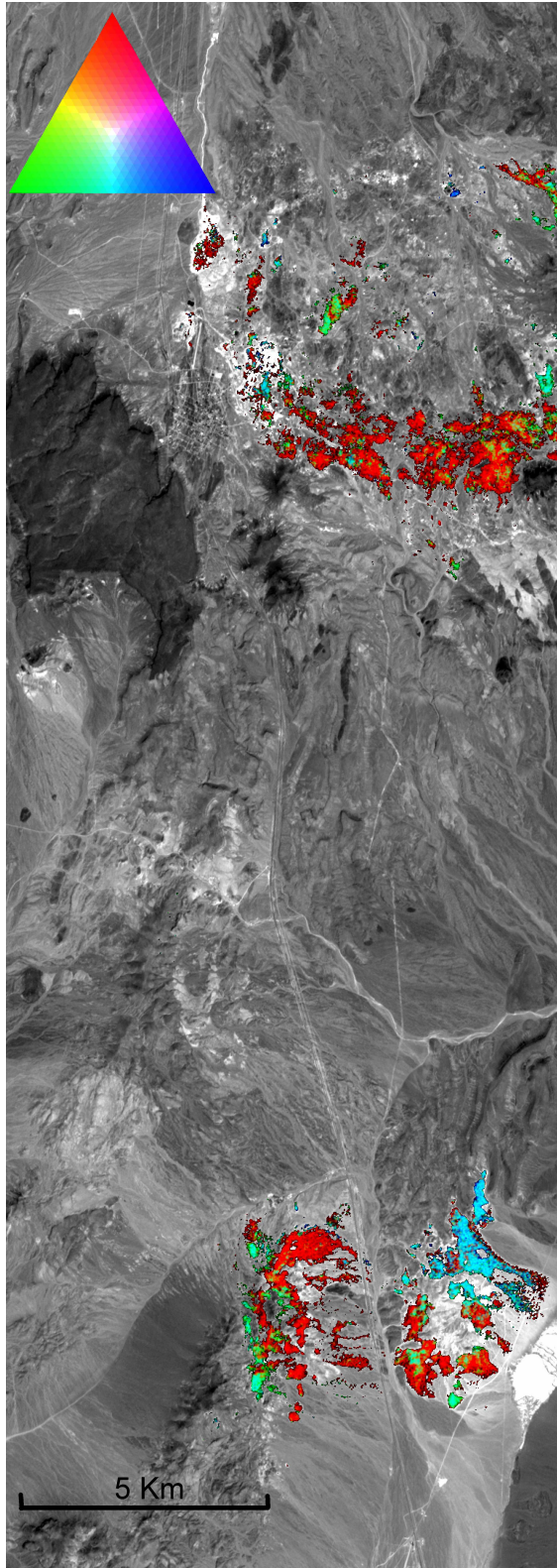


Figure 20: Results of ASTER analysis for the Goldfield and Cuprite areas in Nevada. The image maps alunite, kaolinite, and illite responses as RGB.

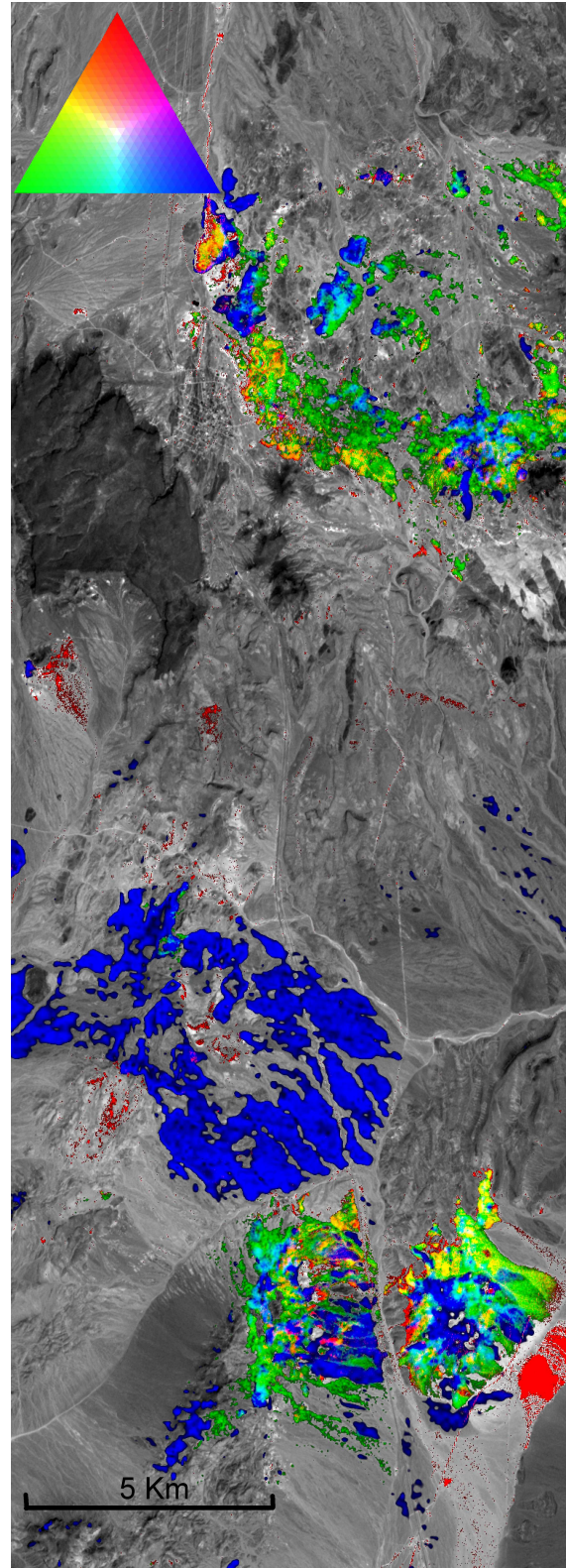


Figure 21: Results of ASTER analysis for the Goldfield and Cuprite areas in Nevada. The image maps iron oxide, clay, and quartz responses as RGB.

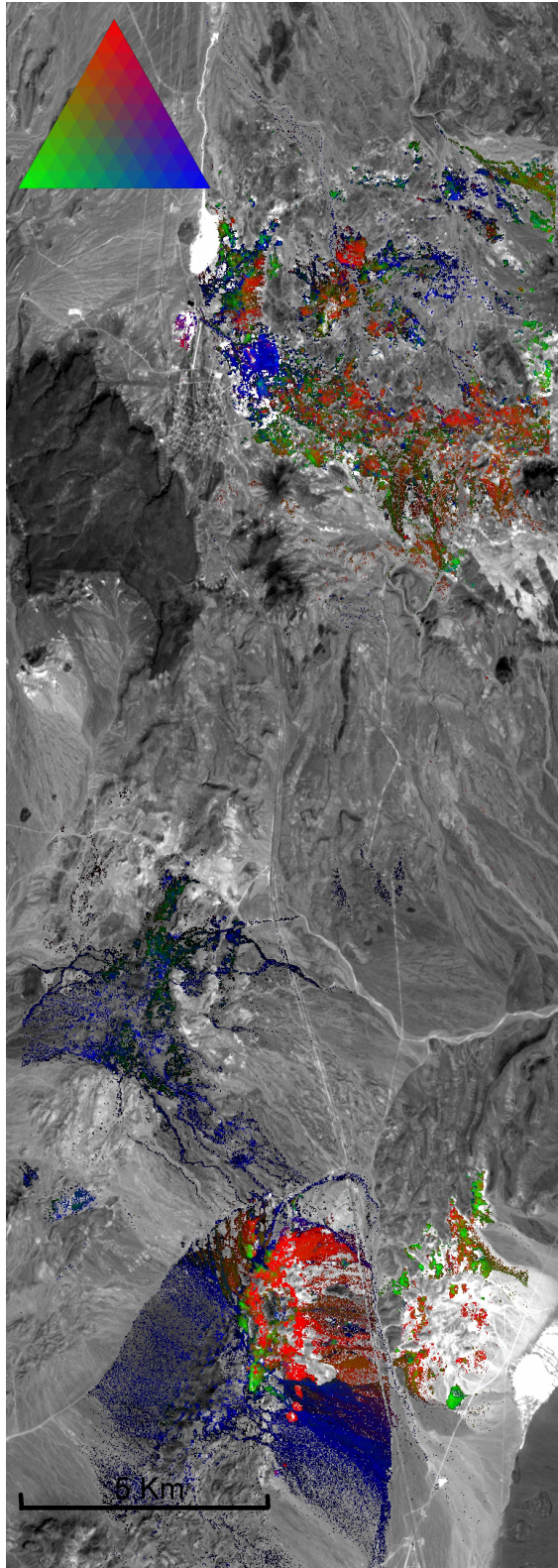


Figure 22: AVIRIS unmixing results (OCCM) for the Goldfield and Cuprite areas in Nevada. The image shows alunitic, kaolinitic, and illitic as RGB.

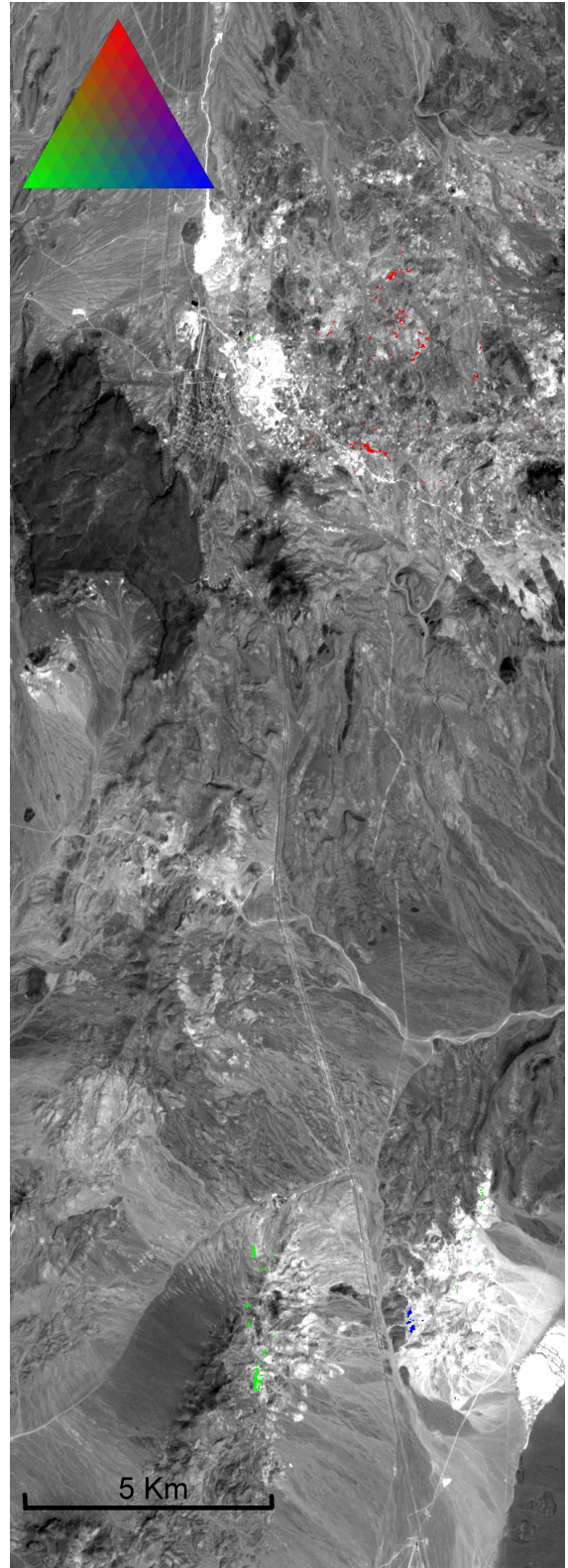


Figure 23: AVIRIS unmixing results (OCCM) for the Goldfield and Cuprite areas in Nevada. The image shows minor occurrences of pyrophyllite, dickite, and buddingtonite as RGB.

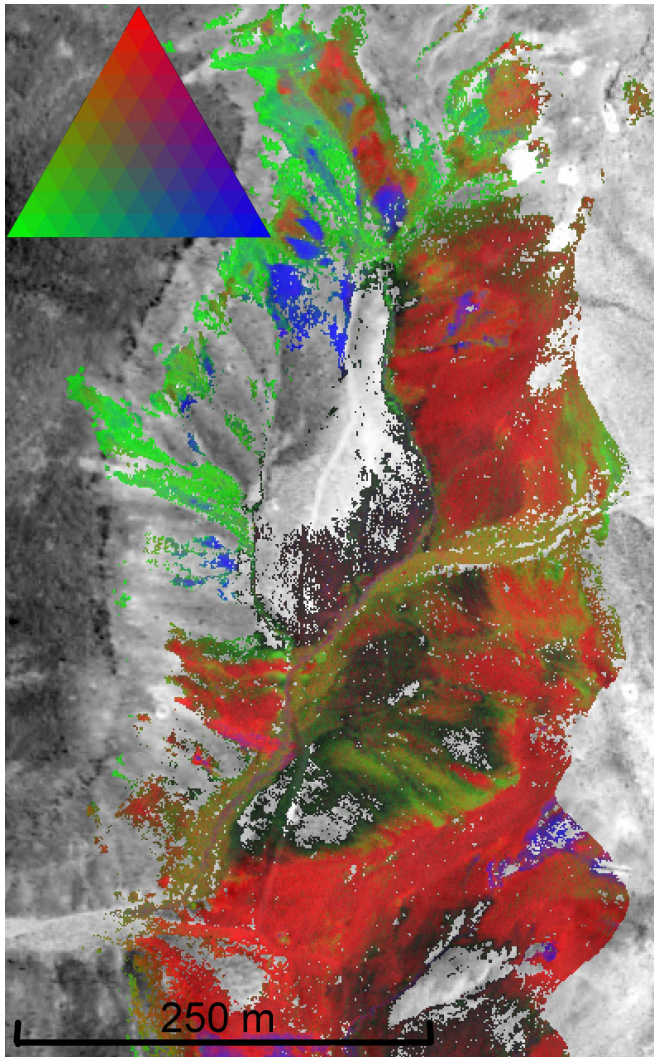


Figure 24: High spatial resolution (1 meter) hyperspectral results for the “Buddintonite Bump” area of Cuprite, Nevada. The image maps alunite, kaolinite, and illite as RGB. Data where acquired by Spectir LLC. Using a AISA Dual imaging spectrometer.

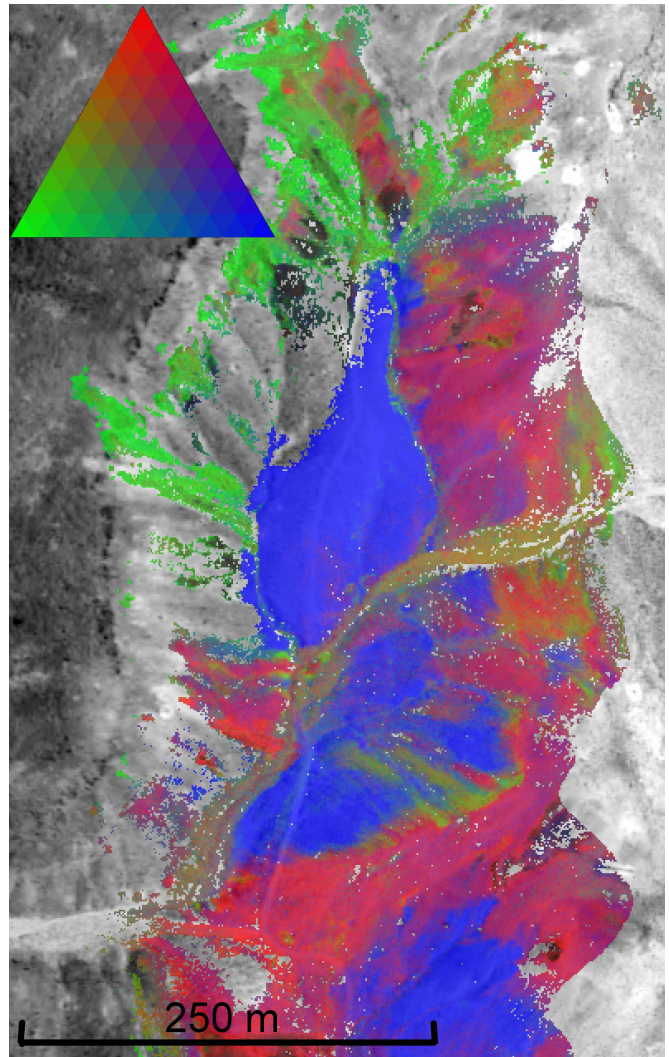


Figure 25: High spatial resolution (1 meter) hyperspectral results for the “Buddintonite Bump” area of Cuprite, Nevada. The image maps alunite, kaolinite, and buddingtonite as RGB. Data where acquired by Spectir LLC. using an AISA Dual imaging spectrometer.

REFERENCES

Adler-Golden, S. Berk, A., Bernstein, L.S. Richtsmeier, S. et al. 1998; “Flash, A MODTRAN4 Atmospheric Correction Package for Hyperspectral Data Retrievals and Simulations” AVIRIS Proceedings: 1998, JPL Publication 97-21.

Agar, R.A., 1994. “Geoscan Airborne Multi-Spectral Scanners as Tools in Exploration for Western Australian Diamond and Gold Deposits.” In:- Dentith, M., Groves, D., Trench, A., & Frankcombe, K, (eds), “Geophysical Signatures of Western Australian Mineral Deposits”, The University of Western Australia, Publication No.26, pp435-447.

Agar, R.A., 1999; Spectral and Mineralogical Characterisation of Alteration Associated with Hydrocarbon Seepage Using Geoscan AMSS MKII Data Over Palm Valley, Australia. Proc. 13th

International Conference on Applied Geologic Remote Sensing, Vancouver, VI, pp1-110 – 117.

Agar, R.A. and R. Villanueva. 1997. Satellite, Airborne and Ground Spectral Data Applied to Mineral Exploration in Peru. Proc. 12th International Conference on Applied Geologic Remote Sensing, Denver, VI, pp13-20.

Boardman, J.W. 1989. Inversion of imaging spectrometry data using singular value decomposition. In Proc. IGARSS 89, 12th Canadian Symposium on Remote Sensing. 4:2069-2072.

Anderson, J.A., 1982, Characteristics of leached capping and techniques of appraisal, in Titley, S.R., 1982, Advances in Geology of the Porphyry Copper Deposits, Southwestern North America: Tucson, Arizona, The University of Arizona Press, p. 275-294.

Boardman, J.W. 1989. Inversion of imaging spectrometry data using singular value decomposition. In Proc. IGARSS 89, 12th Canadian Symposium on Remote Sensing. 4:2069-2072.

- Boardman, J.W., F.A. Kruse, and R.O. Green. 1995. Mapping target signatures via partial unmixing of AVIRIS data. In Proceedings, Sixth AVIRIS Airborne Geoscience Workshop. JPL Publication 95-1. 1:23-26.
- Borel, C.C. & . Schlapfe, D. 1996; Atmospheric Pre-Corrected Differential Absorption Techniques to Retrieve Columnar Water Vapor: Theory and Simulations. AVIRIS Proceedings: 1996, JPL Publication 96-4, pp13-21.
- Carvalho, A.C. and P.R. Meneses. 2000. Spectral correlation mapper (SCM): an improvement on the spectral angle mapper (SAM). In Proceedings, Tenth AVIRIS Airborne Geoscience Workshop. JPL Publication 00-18.
- Chen, P.H., Lin, C.J., and Schölkopf, B. 2003. A tutorial. <http://www.csie.ntu.edu.tw/~cjlin/papers/nusvmtutorial.pdf>. (Accessed 3/21/2007).
- Christianini, N. 2001. Support vector and kernel machines – ICML '01 Tutorial. The Eighteenth International Conference on Machine Learning, June 28 – July 1, 2001. Williams College, Massachusetts.
- Clark, R.N. 1983. Spectral properties of mixtures of montmorillonite and dark carbon grains: Implications for remote sensing minerals containing chemically and physically adsorbed water. *J. Geophys. Res.* 88:10635-10644.
- Clark, R.N., A.J. Gallagher, and G.A. Swayze. 1990. Material absorption band depth mapping of imaging spectrometer data using a complete band shape least-squares fit with library reference spectra. In Proceedings, Second AVIRIS Airborne Geoscience Workshop. JPL Publication 90-54.
- Clark, R.N., G.A. Swayze, T.V.V. King, K.E. Livo, J.B. Dalton, and R.F. Kokaly. 1999. Tetracorder and expert system feature identification rules for reflectance (and emittance) spectroscopy analysis 1: Visible to near-infrared detection of minerals, organics, vegetation, water, amorphous and other materials. In Proceedings, Ninth AVIRIS Airborne Geoscience Workshop. JPL Publication 99-17.
- Clark, R.N., G.A. Swayze, K.E. Livo, R.F. Kokaly, T.V.V. King, J.B. Dalton, J.S. Vance, B.W. Rockwell, T. Hoefen, and R.R. McDougal. 2002. Surface reflectance calibration of terrestrial imaging spectroscopy data: a tutorial using AVIRIS. In Proceedings, Twelfth AVIRIS Airborne Geoscience Workshop. JPL Publication in press. Pre-press copy from: ftp://popo.jpl.nasa.gov/pub/docs/workshops/02_docs/toc.html. (Accessed 9/29/2006).
- Cocks T. D., Jenssen, R., Stewart, A., Wilson, I., and Shields, T., 1998. The HyMap Airborne Hyperspectral Sensor: The system, calibration and performance. 1st EARSEL Workshop on Imaging Spectrometry, 6-8th October, Zurich, 1998.
- Collins, W. & Chang, S., 1990. The Geophysical Environmental Research Corp. 63 Channel Airborne Imaging Spectrometer and 12 Band Thermal Scanner. *Proc. SPIE.* 1298:62-71.
- Coulter, D., 2002. ASTER Problems and Resolutions; A Data User's Perspective. Presented to "ASTER Unveiled," Annual General Meeting of the Geological Remote Sensing Group, Geological Society of London, December 2002.
- Coulter, D.W. 2006. Remote sensing analysis of alteration mineralogy associated with natural acid drainage in the Grizzly Peak Caldera, Sawatch Range, Colorado. Unpublished Ph.D. dissertation. Golden, Colorado. Colorado School of Mines. p 146.
- Crosta, A. and J.M. Moore. 1989. Enhancement of Landsat Thematic Mapper imagery for residual soil mapping in SW Minas Gerais State, Brazil: a prospecting case history in Greenstone belt terrain. In: Proceedings of the 7th ERIM Thematic Conference: Remote sensing for exploration geology, pp. 1173-1187.
- Cudahy, T.J. & Ramaidou, E., 2004: Mine Face and Bench Scanning; Spectral Mine Imaging. In: Spectral Sensing for Mineral Exploration; Workshop 2, 12th Australasian Remote Sensing & Photogrammetry Conference, Fremantle, Western Australia.
- Cudahy, T.J., Okada, K. & Brauhart, C., 2000. Targeting VMS-style Zn mineralisation at Panorama, Australia, using airborne hyperspectral VNIR-SWIR HYMAP data. ERIM Proceedings of the 14th International Conference on Applied Geologic Remote Sensing, 6-8 November, Las Vegas, pp. 395-402.
- Cudahy, T.J., Hewson, R.D., Huntington, J.F., Quigley, M.A., and Barry, P.S., 2001. The performance of the satellite-borne Hyperion Hyperspectral VNIR-SWIR imaging system for mineral mapping at Mount Fitton, South Australia. Proceedings IEEE 2001 International Conference on Geoscience and Remote Sensing, Sydney 9-13 July.
- De Backer, S., P. Kempeneers, W. Debruyne, P. Scheunders. 2005. A band selection technique for spectral classification. *IEEE Geoscience and Remote Sensing Letters.* 2 (3): 319-323.
- Duda, K.A., 2004; ASTER and MODIS Data at the NASA Land Processes Distributed Active Archive Center. Proceedings, 12th Australasian Remote Sensing & Photogrammetry Conference, Fremantle, Western Australia.
- Farr, T. & Kobrick, M. 2000. The Shuttle Radar Topography Mission. Proceedings IEEE 2000 International Geoscience and remote sensing Symposium.
- Farrand, W.H. 2001. Analysis of AVIRIS data: A comparison of the performance of commercial software with published algorithms. In Proceedings, Eleventh AVIRIS Airborne Geoscience Workshop. JPL Publication 02-1.
- Farrand, W.H. and J.C. Harsanyi. 1997. Mapping the distribution of mine tailings in the Coeur d'Alene River Valley, Idaho through the use of a constrained energy minimization technique. *Remote Sens. Env.* 59:64-76.
- Fraser, S.J. & Green, A.A. 1987. Software defoliant for geological analysis of band ratios. *International Journal of Remote Sensing* V8, No.3, pp525-532.
- Green, A.A and M.D. Craig. 1985. Analysis of aircraft spectrometer data with logarithmic residuals. Jet Propulsion Laboratory, Pasadena, CA. JPL Publication 85-41, pp. 111-119.
- Green, A.A., M. Berman, P. Switzer, and M.D. Craig. 1988. A transformation for ordering multispectral data in terms of image quality with implications for noise removal. *IEEE Transactions on Geoscience and Remote Sensing.* 26(1):65-74.
- Hapke, B. 1993. *Theory of Reflectance and Emittance Spectroscopy.* Cambridge University Press, Cambridge, UK, 455 p.
- Harris, P.D., Winkler, K.S. & Sears, M., 2006. Hyperspectral Imaging of Drillcore – How and Why? Unpublished presentation to AMIRA, July 2006.
- Harsanyi, J.C. and C.I. Chang. 1994. Hyperspectral image classification and dimensionality reduction: An orthogonal subspace projection approach. *IEEE Transactions on geosciences and remote sensing.* 32(4):779-785.

- Hauff, P.L. 2004; Field Spectroscopy. In: Spectral Sensing for Mineral Exploration; Workshop 2, 12th Australasian Remote Sensing & Photogrammetry Conference, Fremantle, Western Australia.
- Hauff, P.L., 2005. Remote Sensing of the Alteration System at Virginia City, Nevada. In: Remote Sensing Short Course Geological Society of Nevada, Symposium. Reno, Nevada and Spectral International Inc.
- Hausknecht P., Flack J.C., Huntington J.F, Mason P., Boardman J.W., 1999. Hyperspectral profiling versus imaging: A mineral mapping case study to evaluate the OARS concept. Proceedings 13th Thematic Conference Geologic Remote Sensing, Vancouver, Canada, Vol. I, pp. 529-536.
- Hausknecht, P., Whitbourn, L.B, Connor, P., Flack, J., Huntington, J.F., Hewson, R., and Batty, S. 2000. OARS Hyperspectral Surface Mapping Simultaneously with Airborne Geophysics. In Tenth Australasian Remote Sensing and Photogrammetry Conference Proceedings, Adelaide, pp. 259-267.
- Hausknecht, P., Cudahy, T., Jurza, P., & Yajima, T., 2004. The Airborne ARGUS Line-Profiling System: Integrated Hyperspectral VNIR-SWIR-TIR Spectrometry with Magnetism and Radiometrics - Geological Case History, Panorama, Pilbara Western Australia. Proceedings, 12th Australasian Remote Sensing & Photogrammetry Conference, Fremantle, Western Australia.
- Hensley, S., Rosen, P. & Gurrola, E., 2000. Topographic map generation from the Shuttle Radar Topography Mission C-band SCANSAR Interferometry. Proceedings of the Asia Pacific Meeting, SPIE, 2000, Sendai.
- Hewson, R.D., Cudahy, T.J., & Huntington, J.F., 2001. Geologic and alteration mapping at Mt Fitton, South Australia, using ASTER satellite-borne data. Proceedings IEEE 2001 International Geoscience and remote sensing Symposium, 9-13 July. 3pp.
- Hussey, M.C., 2004. Operational Application of the De Beers Hyperspectral Scanner. Proceedings, 12th Australasian Remote Sensing & Photogrammetry Conference, Fremantle, Western Australia; pp459-486.
- Ientilucci, E. 2001. Hyperspectral image classification using orthogonal subspace projections: image simulation and noise analysis. Rochester Institute of Technology, Center for Imaging Science. http://www.cis.rit.edu/~ejipci/Reports/osp_paper.pdf (Accessed 4/2/2007).
- Iwasaki, A., Fujisada, H., Akao, H., Shindou, O., and Akagi, S., 2001. Enhancement of spectral separation performance for ASTER/SWIR. Proceedings of SPIE - The International Society for Optical Engineering, 4486: 42-50.
- JPL, 1987. AVIRIS Organisation & Tasks. JPL Publication 87-38.
- Kruse, F.A. 1998. Advances in Hyperspectral Remote Sensing for Geologic Mapping and Exploration. Proceedings 9th Australasian Remote Sensing & Photogrammetry Conference, Sydney.
- Kruse, F.A., A.B. Lefkoff, J.W. Boardman, K.B. Heidebrecht, A.T. Shapiro, P.J. Barloon, and A.F.H. Goetz. 1993. The Spectral Image Processing System (SIPS) - interactive visualization and analysis of imaging spectrometer data. Remote Sensing of Environment, Special Issue on AVIRIS. 44:145-163.
- Kruse, F.A., Boardman, J.W. & Huntington, J.F., 2002. Hyperion Validation Results for Mineral Mapping. Final Report, NASA Grant NCC5-495.
- Landgrebe, D.A. 2003. Signal Theory Methods in Multispectral Remote Sensing, John Wiley and Sons, Inc., Hoboken, New Jersey, USA, 508 p.
- Linton, P., Honey, F., Harris, P.D., Winkler, K.S. & Sears, M., 2004. Experimental Automated Spectral Core Imaging System For Mineral Identification. Proceedings, 12th Australasian Remote Sensing & Photogrammetry Conference, Fremantle, Western Australia.
- Lipton, G. 1997. Spectral and microwave remote sensing: an evolution from small scale regional studies to mineral mapping and ore deposit targeting. Geophysics and geochemistry at the millennium: Proceedings of Exploration 97 Fourth Decennial International Conference on Mineral Exploration. Toronto, Canada.
- Loughlin, W. P., 1991. Principal component analysis for alteration mapping. Photogrammetric Engineering and Remote Sensing. 57: 1163-1169.
- van der Meer, F.D. 2000. Imaging spectrometry for geological applications. Encyclopedia of Analytical Chemistry, Applications of Instrumental Methods, Remote Sensing. (R.A. Meyers gen. ed., P.M. Mather section ed.). J. Wiley & Sons Ltd. Chichester, UK.
- Mauger, A.J., Keeling, J.L. & Huntington, J.F., 2004. Inging Remote Sensing Down To Earth: CSIROHylogger As Applied In The Tarcoola Goldfield, South Australia. Proceedings, 12th Australasian Remote Sensing & Photogrammetry Conference, Fremantle, Western Australia.
- Neville, R.A., Rowlands, N., Marois, R. & Powell, I., 1995. SFSI: Canada's First Airborne SWIR Imaging Spectrometer. Canadian Journal of Remote Sensing, Vol. 21, No. 3, pp. 328-336.
- Pavez, A. & Agar, R.A., 2001. Mineral Indices Derived From Geoscan Amss Data As A Mapping And Exploration Tool; The Chañarcillo Skarn District, Chile. Proc. International Geoscience & Remote Sensing Symposium, Sydney, July 2001.
- Pontual, S., 2004. Approaches to Spectral Analysis and its Application to Exploration & Mining. In: Spectral Sensing for Mineral Exploration; Workshop 2, 12th Australasian Remote Sensing & Photogrammetry Conference, Fremantle, Western Australia.
- Pratt, W.K. 2001. Digital Image Processing, Third Edition. John Wiley and Sons, Inc. New York.
- Prelat, A.E. & Chang, S-H, 1997. TEEMS: Texaco Energy and Environmental Multispectral Imaging Spectrometer. Proc. American Society for Photogrammetry and Remote Sensing, "Land Satellite Information in the Next Decade II: Sources and Applications," Dec. 1997, Washington D.C.
- Quigley, M., Huntington, J., Whitbourn, K. L., Connor, W., Howard, D. and Phillips, R., 2004. The CSIRO HyLogger. In: Spectral Sensing for Mineral Exploration; Workshop 2, 12th Australasian Remote Sensing & Photogrammetry Conference, Fremantle, Western Australia.
- Reuter, D., McCabe, G., Dimitrov, R., Graham, S., Jennings, D., Matsumura, M., Rapchun, D. & Travis, J., 2001. The LAISA/Atmospheric Corrector (LAC) on EO-1 Proceedings IEEE 2001 International Conference on Geoscience and Remote Sensing, Sydney 9-13 July.
- Rowan, L. C. and Mars, J.C., 2003. Lithologic mapping in the Mountain Pass, California area using Advanced Spaceborne Thermal Emission and reflection radiometer (ASTER) data. Remote Sensing Environment, 84: 350-366.

- Rowan, L. C., Hook, S. J., Abrams, M. J., & Mars, J. C., 2003, Mapping hydrothermally altered rocks at Cuprite, Nevada, using the Advanced Spaceborne Thermal Emission and Reflection Radiometer (ASTER), a new satellite-imaging system. *Economic Geology*, 98, pp. 1019-1027.
- Rowan, L.C., P.H. Wetlaufer, A.F.H. Goetz, F.C. Billingsley, J.H. Stewart. Discrimination of rock types and detection of hydrothermally altered areas in south-central Nevada by use of computer-enhanced ERTS images. Geological Survey Professional Paper 883, United States Geological Survey, U.S. Government Printing Office, Washington D.C.
- RSI 2005. ENVI User's Guide – 4.2. Research Systems Incorporated. Boulder, Colorado.
- Sarture, C.M., Chovit, C.J., Chrien, T.G., Eastwood, M.L., Green, R.O., & Kurzweil C.G., 1998. The AVIRIS Low Altitude Option - An Approach to Increase Geometric Resolution and Improve Operational Flexibility Simultaneously. AVIRIS Proceedings: 1998, JPL Publication 97-21.
- Schowengerdt, R.A. 1997. Remote Sensing Models and Methods for Image Processing 2nd Edition. Academic Press. 522 p.
- Staenz K., Neville, R., Lévesque, J., Szeredi, T., Singhroy, V., Borstad, G. & Hauff, P., 1999. Evaluation of CASI and SFSI Hyperspectral Data for Environmental and Geological Applications — Two Case Studies. *Canadian Journal of Remote Sensing*, Vol. 25, No 3, 1999, pp. 311-322.
- Thompson, A.J.B., Hauff, P.L. & Robitaille, A.J., 1999. Alteration Mapping in Exploration: Application of Short-Wave Infrared (SWIR) Spectroscopy. *Econ. Geol. Newsletter*, #39, October 1999.
- Toutin, T., 2001. DEM Generation from New VNIR Sensors: IKONOS, ASTER and Landsat-7. Proceedings IEEE 2001 International Geoscience and remote sensing Symposium, 9-13 July.
- Vane, G., Green, R.O., Chrien, T.G., Enmark, H.T., Hansen, E.G. & Porter, W.M., 1993. The Airborne Visible/Infrared Imaging Spectrometer (AVIRIS). *Remote Sensing of Environment*, Vol. 44, pp. 127-143.
- Watanabe, H., 2002. Current Status of ASTER, ASTER Ground Data System and its Application. Presented to "ASTER Unveiled," Annual General Meeting of the Geological Remote Sensing Group, Geological Society of London, December 2002.
- Watanabe, H., 2004. Performance of ASTER Sensor, ASTER Product Information and Recent Topics. Proceedings, 12th Australasian Remote Sensing & Photogrammetry Conference, Fremantle, Western Australia.
- Wikipedia (2007): http://en.wikipedia.org/wiki/Google_Earth